produced by γ-secretase, in the presence or absence of CA-074Me (Supplemental Fig. S2).

In addition, we treated γ-secretase-deficient *PS1*$^{-/-}$ *PS2*$^{-/-}$ cells with CA-074Me. Western blot analysis with an anti-APP antibody showed that CTFα significantly accumulated in *PS1*$^{-/-}$*PS2*$^{-/-}$ cells following CA-074Me treatment (Fig. 5*C, D*). From these results, we concluded that cathepsin B had no effect on the production of CTFs from APP, and cathepsin B degrades CTFs independently of γ-secretase.

### Cathespin B degrades AICD *in vitro*

To examine whether AICD is directly degraded by cathepsin B, we subjected synthetic AICD to increasing quantities of purified cathepsin B for 60 min either in the absence or presence of CA-074 (**Fig. 6**). AICD degradation was assessed by Western blot using an anti-APP antibody. AICD was efficiently degraded by cathepsin B. This degradation by cathepsin B was promptly abolished by CA-074.

### γ-Secretase prefers to degrade phosphorylated APP, whereas cathepsin B processes all APP substrates in the same way

Our above results indicate that cathepsin B contributes to the degradation of both CTFs and AICD independently of γ-secretase. We hypothesized that there was a regulatory factor for proteolysis of CTFs by cathepsin B or γ-secretase. A previous study demonstrated that CTFs phosphorylated at Thr668 facilitate their own processing by γ-secretase (22). We treated $APP_{NL}$-H4 cells with CA-074Me, β-secretase inhibitor IV, or L-685,458, and then assessed the levels of phosphorylated CTFs (pCTFs) and total CTFs containing phosphorylated and nonphosphorylated CTFs (npCTFs) (**Fig. 7*A, B***). We used CTFs containing CTFα and CTFβ, both of which are γ-secretase substrates. In the case of treatment with CA-074Me or β-secretase inhibitor IV, the ratios of the accumulated pCTFs to total CTFs did not show a significant difference. In contrast, the γ-secretase inhibitor L-685,458 caused an increase in this ratio. This significant increase in phosphorylated CTFs means that treatment with L-685,458, unlike treatment with CA-074Me, caused the increased accumulation of pCTFs over npCTFs.

To discern the difference between pCTFs and npCTFs for γ-secretase activity, we established a cell line that stably overexpressed APP mutated at a phosphorylation site (Thr to Ala on 668; $APP_{NL\_TA}$-H4 cells) and then compared the accumulation rate of CTFs in $APP_{NL}$-H4 cells with that in $APP_{NL\_TA}$-H4 cells (Fig. 7*C, D*). Although treatment with CA-074Me caused an increase in CTFs in both $APP_{NL}$-H4 cells and $APP_{NL\_TA}$-H4 cells as compared to vehicle treatment in each cell, there was no significant difference in the accumulation rate of CTFs between $APP_{NL}$-H4 cells and $APP_{NL\_TA}$-H4 cells. In contrast, treatment with L-685,458 caused accumulation of CTFs in both $APP_{NL}$-H4 cells and $APP_{NL\_TA}$-H4 cells as compared to vehicle treatment in each cell, and the accumulation rate of CTFs in $APP_{NL}$-H4 cells was 4.5 times larger than that in $APP_{NL\_TA}$-H4 cells. From these data, we could conclude that cathepsin B catalyzed the proteolysis of CTFs regardless of APP phosphorylation, whereas γ-secretase preferred pCTFs to npCTFs.

## DISCUSSION

Cathepsin B, a well-characterized endosomal/lysosomal cysteine protease in mammalian cells, plays major roles in intracellular protein proteolysis (23, 24). Its specific inhibitor CA-074Me is a membrane-permeable analog of CA-074 that inhibits intracellular cathepsin B. CA-074Me is widely used *in vivo* and *in vitro*, although some

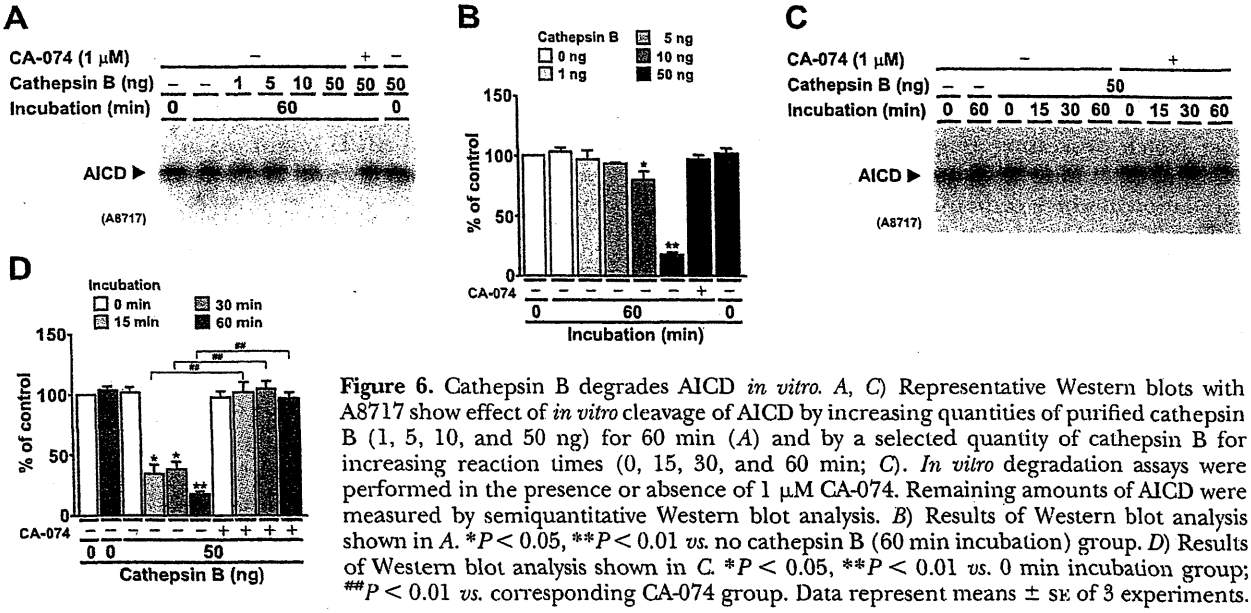


**Figure 6.** Cathepsin B degrades AICD *in vitro*. *A, C*) Representative Western blots with A8717 show effect of *in vitro* cleavage of AICD by increasing quantities of purified cathepsin B (1, 5, 10, and 50 ng) for 60 min (*A*) and by a selected quantity of cathepsin B for increasing reaction times (0, 15, 30, and 60 min; *C*). *In vitro* degradation assays were performed in the presence or absence of 1 μM CA-074. Remaining amounts of AICD were measured by semiquantitative Western blot analysis. *B*) Results of Western blot analysis shown in *A*. $^{*}P < 0.05$, $^{**}P < 0.01$ *vs.* no cathepsin B (60 min incubation) group. *D*) Results of Western blot analysis shown in *C*. $^{*}P < 0.05$, $^{**}P < 0.01$ *vs.* 0 min incubation group; $^{\#\#}P < 0.01$ *vs.* corresponding CA-074 group. Data represent means ± SE of 3 experiments.

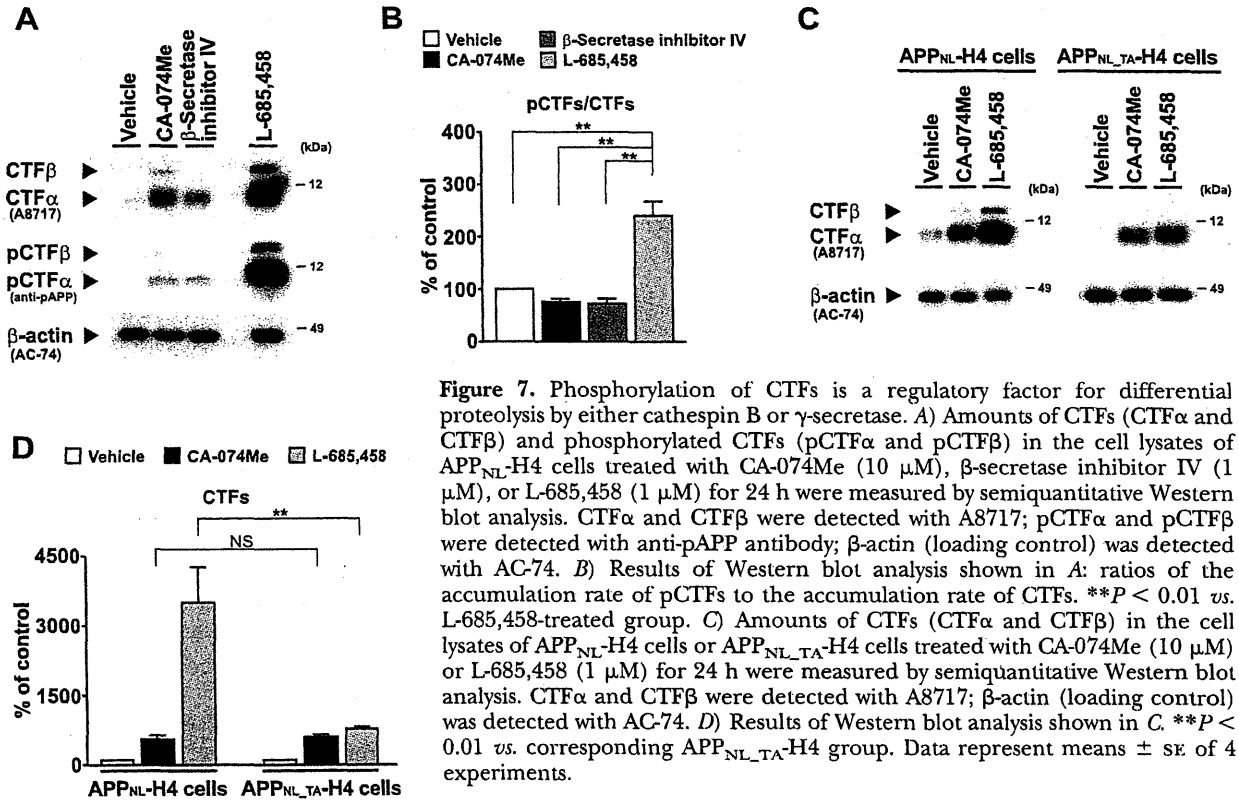


**Figure 7.** Phosphorylation of CTFs is a regulatory factor for differential proteolysis by either cathespin B or γ-secretase. *A*) Amounts of CTFs (CTFα and CTFβ) and phosphorylated CTFs (pCTFα and pCTFβ) in the cell lysates of $APP_{NL}$-H4 cells treated with CA-074Me (10 μM), β-secretase inhibitor IV (1 μM), or L-685,458 (1 μM) for 24 h were measured by semiquantitative Western blot analysis. CTFα and CTFβ were detected with A8717; pCTFα and pCTFβ were detected with anti-pAPP antibody; β-actin (loading control) was detected with AC-74. *B*) Results of Western blot analysis shown in *A*: ratios of the accumulation rate of pCTFs to the accumulation rate of CTFs. $^{**}P < 0.01$ *vs.* L-685,458-treated group. *C*) Amounts of CTFs (CTFα and CTFβ) in the cell lysates of $APP_{NL}$-H4 cells or $APP_{NL\_TA}$-H4 cells treated with CA-074Me (10 μM) or L-685,458 (1 μM) for 24 h were measured by semiquantitative Western blot analysis. CTFα and CTFβ were detected with A8717; β-actin (loading control) was detected with AC-74. *D*) Results of Western blot analysis shown in *C*. $^{**}P < 0.01$ *vs.* corresponding $APP_{NL\_TA}$-H4 group. Data represent means ± SE of 4 experiments.

studies suggest that CA-074Me deprives the specificity of cathepsin B by methyl esterification, to distinguish between inhibition of cathepsin B and that of other cysteine proteases, such as cathepsins H, L, and calpains (12–15). In the present study, we have demonstrated that cathepsin B possesses two novel roles in the metabolism of APP using a pharmacological approach with CA-074Me. Although chloroquine or $NH_4Cl$ treatment has been reported to cause accumulation of both CTFs and AICD, which are a substrate and product of γ-secretase (11), CTFs have been recognized to be a substrate of only γ-secretase (1–4). As shown here, however, CTFs are also a substrate of cathepsin B; cathepsin B degraded CTFs with or without Swedish FAD mutation of APP independently of γ-secretase (Figs. 1, 2, and 5 and Supplemental Fig. S1) but did not affect Notch processing (Fig. 4). The key regulatory factor to determine an alternative pathway of CTF degradation in which cathepsin B or γ-secretase may be involved is phosphorylation at Thr668 of APP (Fig. 7). In addition, cathepsin B is also involved in degradation of AICD (Figs. 1, 2, and 6 and Supplemental Figs. S1 and S3).

The organelles in which cathepsin B degrades CTFs and AICD are a critical issue. In the hippocampal CA1 pyramidal neurons in mice, cathepsin B is primarily localized in the lysosomes and early endosomes (25). In the lysosome, one model posits that a KFERQ-like motif in APP, which is a specific pentapeptide lysosome-targeting consensus sequence (26), is recognized by a complex of chaperone proteins (including the heat shock 73-kDa protein, Hsc73) and then targeted to the lysosomal membrane for binding to LAMP2a, followed by transportation into the lysosomal lumen for degradation (27). Alternatively, Hsc73 binds to APP at another site unrelated to KFERQ sequence (28). However, in the early endosome, it is also possible that cathepsin B directly encounters CTFβ and AICD, which has been freshly produced, and degrades them. APP interacts with β-secretase [β-site APP-cleaving enzyme (BACE)] at the cell surface and then appears to be internalized together into early endosomes, undergoing β-cleavage (29), and PS also localizes in the early endosome, generating Aβ and AICD (30). On the other hand, because CTFα is thought to be produced by α-secretase at the cell surface (31), CTFα might be led to the lysosome by Hsc73, and thus be degraded by cathepsin B. Cathepsin B-mediated degradation of CTFα, CTFβ, and AICD might occur in different subcellular compartments and be regulated by different signaling.

The mode of regulation of cathepsin B activity remains unclear. Putative models include an endogenous cysteine protease inhibitor cystatin C (32) and a feedback mechanism based on AICD. AICD is assumed to function as a transcription activating factor for targeting *APP*, *BACE*, and *neprilysin* genes (33, 34). If gene expression of *APP* and *BACE* is up-regulated by AICD, Aβ levels should be increased. The major Aβ-degrading enzyme neprilysin, which is also likely to be upregulated, regulates levels of Aβ. Aβ42 activates cathepsin B (25), and then cathepsin B degrades CTFs and AICD to regulate transcription *via* AICD. An alternative name for cathepsin B is APP secretase (APPS), and it has been

suggested that cathepsin B is involved in proteolysis of FL-APP. Although it was initially demonstrated that cathepsin B has α-secretase-like activity through experiments with an artificial substrate that mimicked the α-secretase cleavage site (35), Hook *et al.* (14) showed that cathepsin B functioned as a β-secretase in the regulated secretory pathway against wild-type but not the Swedish mutation of APP. Moreover, it has been reported that cathepsin B has Aβ-degrading activity *in vivo* and *in vitro*, reducing the amount of amyloid plaques in aged AD model mice by lentivirus-mediated expression of cathepsin B (25). In the present study, cathepsin B seems to have no α- or β-secretase activity, and it may contribute to some Aβ degradation. However, cathepsin B is likely to be a multifunctional enzyme for APP metabolism; further studies are needed to establish its role in APP processing. First, for understanding the contribution of cathepsin B as β-secretase, it is important to estimate a ratio between Aβ present in the regulated secretory pathway and Aβ present in the constitutive secretory pathway in normal or AD brain. Second, from a different perspective, because treatment with CA-074Me results in acute inhibition of cathepsin B, there is no denying that a pharmacological approach with CA-074Me results in a different outcome than a genetic knockout experiment. As indicated above, cathepsin B-deficient mice exhibit no obvious phenotype, including the amounts of CTFs (25, 36); however, it has been suggested that cathepsin L compensates for the deficiency of cathepsin B. In this study, the treatment with E-64d, which is a broad cysteine protease inhibitor, caused accumulation of CTFα, CTFβ, and AICD. In cases in which CA-074Me loses the specificity of cathepsin B, cathepsin L also might be involved in degradation of CTFα, CTFβ, and AICD. Cathepsin B and L double-knockout mice are terminal during the second to fourth week of life and show neuronal loss (37). Although it has been reported that cathepsin B produces CTFβ in the regulated secretory pathway (14, 38, 39), our study clearly showed that cathepsin B degrades both CTFs and AICD. Since CTFs themselves are toxic (40) and AICD transgenic mice display age-dependent neurodegeneration (41), it may not be advisable to inhibit cathepsin B activity to treat AD, which may worsen rather than improve AD.

Protein phosphorylation, in particular, plays a significant role in a wide range of molecular and cellular biology. Reversible phosphorylation of proteins is an important regulatory mechanism that may influence conformational changes in the structure, altered localization, and enzymatic activity regulation. Phosphorylation of APP has been previously reported to induce a conformational change in the cytoplasmic region to alter interaction with Fe65, a neuronal-specific adaptor protein (42). The transfection of APP containing a Thr to Glu mutation (mimics phosphorylation) with Fe65 increases Aβ levels (42). Phosphorylation by stress-induced c-Jun N-terminal kinase (JNK) enhances proteolysis of pCTFs by γ-secretase (22). Although further investigation of the relationship between phosphorylation of APP and cathepsin B is required, we have provided indirect evidence that cathepsin B degrades CTFs at a constant rate without distinction for the phosphorylation state of the CTF (Fig. 7). Interestingly, inhibition of cathepsin B showed no significant difference in Aβ levels in our experimental paradigm (Supplemental Fig. S2). This result indicates that cathepsin B and γ-secretase share CTFs as a substrate but do not compete against each other. However, γ-secretase preferably hydrolyzed pCTFs over npCTFs (Fig. 7). Why inhibition of γ-secretase causes an increase in the ratio of the accumulation rate of pCTFs to the accumulation rate of CTFs and why inhibition of cathepsin B does not show this result are interesting puzzles still to be resolved. The significant decrease in the accumulation rate of CTFs in $APP_{NL\_TA}$-H4 cells, as compared to that in $APP_{NL}$-H4 cells, when the γ-secretase inhibitor L-685,458 was administered confirms that APP phosphorylation regulates proteolysis of CTFs by γ-secretase. Cyclin-dependent kinase-5 (Cdk5), glycogen synthase kinase-3β (GSK-3β), and JNK are believed to phosphorylate APP at Thr668 (43), suggesting that inhibitors of these kinases would be effective drugs in the treatment of AD. Indeed, the GSK-3 inhibitor lithium chloride reduces Aβ levels (44). Kinase inhibitors, unlike γ-secretase inhibitors, would be expected to specifically block γ-cleavage of CTFs derived from APP without inhibition of γ-cleavage of other substrates (44). Furthermore, because these kinases also phosphorylate tau, which is a major component of neurofibrillary tangles, inhibition of these kinases decreases levels of hyperphosphorylated tau, preventing neurodegeneration and neuronal loss without Aβ reduction (45). In addition, based on our results and previous findings, serine/threonine phosphatases are also drug candidates. Protein phosphatase 2A (PP2A) is one of the most important phosphatases in the brain (46). PP2A activity decreases in AD brains (47), suggesting that Aβ is overproduced by activation of γ-secretase. This decreased PP2A activity also promotes phosphorylation of tau (47).

We propose the following model for roles of cathepsin B in APP processing. APP is metabolized by α- and β-secretase to generate CTFα and CTFβ, respectively. γ-Secretase and cathepsin B continuously hydrolyze CTFs; however, γ-secretase prefers the phosphorylated form of CTFs as substrates and then produces AICD from CTFs. pCTFs, npCTFs, and AICD are substrates for cathepsin B.

In summary, the present data demonstrate that cathepsin B contributes to the degradation of CTFs and AICD independently of α-, β-, and γ-secretases and that γ-secretase prefers pCTFs to npCTFs but cathepsin B does not. This study also suggests that reducing this phosphorylation may be a candidate for therapeutic intervention in AD. FJ

The authors thank Dr. Raphael Kopan (Washington University, St. Louis, MO, USA) for providing a plasmid (ΔEMV:

pCS2/Notch$^{\Delta E}$), Dr. Bart De Strooper (Katholieke Universiteit Leuven, Leuven, Belgium) for providing PS1 and PS2 double-knockout MEF *PS1*$^{-/-}$*PS2*$^{-/-}$ cells, and Drs. Taisuke Tomita and Takeshi Iwatsubo (The University of Tokyo, Tokyo, Japan) for providing mNotch$^{\Delta E}$-N2a cells. The authors also thank Dr. Kazumi Ishidoh (Tokushima Bunri University, Tokushima, Japan) for his valuable advice. This work was supported by the Regional Innovation Cluster Program (City Area Type; Central Saitama Area), the Shimabara Science Promotion Foundation, and a Grant-in-Aid for Scientific Research (C; 20590260) from the Japan Society for the Promotion of Science.

## REFERENCES


1. Zheng, H., and Koo, E. H. (2006) The amyloid precursor protein: beyond amyloid. *Mol. Neurodegener.* **1,** 5
2. Marks, N., and Berg, M. J. (2008) Neurosecretases provide strategies to treat sporadic and familial Alzheimer disorders. *Neurochem. Int.* **52,** 184–215
3. Jacobsen, K. T., and Iverfeldt, K. (2009) Amyloid precursor protein and its homologues: a family of proteolysis-dependent receptors. *Cell. Mol. Life Sci.* **66,** 2299–2318
4. Panza, F., Solfrizzi, V., Frisardi, V., Capurso, C., D'Introno, A., Colacicco, A. M., Vendemiale, G., Capurso, A., and Imbimbo, B. P. (2009) Disease-modifying approach to the treatment of Alzheimer's disease: from α-secretase activators to γ-secretase inhibitors and modulators. *Drugs Aging* **26,** 537–555
5. Tomita, T. (2009) Secretase inhibitors and modulators for Alzheimer's disease treatment. *Expert Rev. Neurother.* **9,** 661–679
6. Doerfler, P., Shearman, M. S., and Perlmutter, R. M. (2001) Presenilin-dependent γ-secretase activity modulates thymocyte development. *Proc. Natl. Acad. Sci. U. S. A.* **98,** 9312–9317
7. Dovey, H. F., John, V., Anderson, J. P., Chen, L. Z., de Saint Andrieu, P., Fang, L. Y., Freedman, S. B., Folmer, B., Goldbach, E., Holsztynska, E. J., Hu, K. L., Johnson-Wood, K. L., Kennedy, S. L., Kholodenko, D., Knops, J. E., Latimer, L. H., Lee, M., Liao, Z., Lieberburg, I. M., Motter, R. N., Mutter, L. C., Nietz, J., Quinn, K. P., Sacchi, K. L., Seubert, P. A., Shopp, G. M., Thorsett, E. D., Tung, J. S., Wu, J., Yang, S., Yin, C. T., Schenk, D. B., May, P. C., Altstiel, L. D., Bender, M. H., Boggs, L. N., Britton, T. C., Clemens, J. C., Czilli, D. L., Dieckman-McGinty, D. K., Droste, J. J., Fuson, K. S., Gitter, B. D., Hyslop, P. A., Johnstone, E. M., Li, W.-Y., Little, S. P., Mabry, T. E., Miller, F. D., Ni, B., Nissen, J. S., Porter, W. J., Potts, B. D., Reel, J. K., Stephenson, D., Su, Y., Shipley, L. A., Whitesitt, C. A., Yin T., and Audia, J. E. (2001) Functional gamma-secretase inhibitors reduce beta-amyloid peptide levels in brain. *J. Neurochem.* **76,** 173–181
8. Gu, Y., Misonou, H., Sato, T., Dohmae, N., Takio, K., and Ihara, Y. (2001) Distinct intramembrane cleavage of the β-amyloid precursor protein family resembling γ-secretase-like cleavage of Notch. *J. Biol. Chem.* **276,** 35235–35238
9. Milano, J., McKay, J., Dagenais, C., Foster-Brown, L., Pognan, F., Gadient, R., Jacobs, R. T., Zacco, A., Greenberg, B., and Ciaccio, P. J. (2004) Modulation of notch processing by γ-secretase inhibitors causes intestinal goblet cell metaplasia and induction of genes known to specify gut secretory lineage differentiation. *Toxicol. Sci.* **82,** 341–358
10. Eisele, Y. S., Baumann, M., Klebl, B., Nordhammer, C., Jucker, M., and Kilger, E. (2007) Gleevec increases levels of the amyloid precursor protein intracellular domain and of the amyloid-β-degrading enzyme neprilysin. *Mol. Biol. Cell* **18,** 3591–3600
11. Vingtdeux, V., Hamdane, M., Bégard, S., Loyens, A., Delacourte, A., Beauvillain, J. C., Buée, L., Marambaud, P., and Sergeant, N. (2007) Intracellular pH regulates amyloid precursor protein intracellular domain accumulation. *Neurobiol. Dis.* **25,** 686–696
12. Hook, V. Y., Kindy, M., and Hook, G. (2008) Inhibitors of cathepsin B improve memory and reduce β-amyloid in transgenic Alzheimer disease mice expressing the wild-type, but not the Swedish mutant, β-secretase site of the amyloid precursor protein. *J. Biol. Chem.* **283,** 7745–7753
13. Van Acker, G. J., Saluja, A. K., Bhagat, L., Singh, V. P., Song, A. M., and Steer, M. L. (2002) Cathepsin B inhibition prevents trypsinogen activation and reduces pancreatitis severity. *Am. J. Physiol. Gastrointest. Liver Physiol.* **283,** G794–G800
14. Hook, V., Toneff, T., Bogyo, M., Greenbaum, D., Medzihradszky, K. F., Neveu, J., Lane, W., Hook, G., and Reisine, T. (2005) Inhibition of cathepsin B reduces β-amyloid production in regulated secretory vesicles of neuronal chromaffin cells: evidence for cathepsin B as a candidate β-secretase of Alzheimer's disease. *Biol. Chem.* **386,** 931–940
15. Ha, S. D., Martins, A., Khazaie, K., Han, J., Chan, B. M., and Kim, S. O. (2008) Cathepsin B is involved in the trafficking of TNF-α-containing vesicles to the plasma membrane in macrophages. *J. Immunol.* **181,** 690–697
16. Asai, M., Iwata, N., Tomita, T., Iwatsubo, T., Ishiura, S., Saido, T. C., and Maruyama, K. (2010) Efficient four-drug cocktail therapy targeting amyloid-β peptide for Alzheimer's disease. *J. Neurosci. Res.* **88,** 3588–3597
17. Asai, M., Iwata, N., Yoshikawa, A., Aizaki, Y., Ishiura, S., Saido, T. C., and Maruyama, K. (2007) Berberine alters the processing of Alzheimer's amyloid precursor protein to decrease Aβ secretion. *Biochem. Biophys. Res. Commun.* **352,** 498–502
18. Herreman, A., Serneels, L., Annaert, W., Collen, D., Schoonjans, L., and De Strooper, B. (2000) Total inactivation of γ-secretase activity in presenilin-deficient embryonic stem cells. *Nat. Cell Biol.* **2,** 461–462
19. De Duve, C., de Barsy, T., Poole, B., Trouet, A., Tulkens, P., and Van Hoof, F. (1974) Commentary. Lysosomotropic agents. *Biochem. Pharmacol.* **23,** 2495–2531
20. Gekle, M., Mildenberger, S., Freudinger, R., and Silbernagl, S. (1995) Endosomal alkalinization reduces $J_{max}$ and $K_m$ of albumin receptor-mediated endocytosis in OK cells. *Am. J. Physiol.* **268,** F899–F906
21. Yagishita, S., Morishima-Kawashima, M., Ishiura, S., and Ihara, Y. (2008) Aβ46 is processed to Aβ40 and Aβ43, but not to Aβ42, in the low density membrane domains. *J. Biol. Chem.* **283,** 733–738
22. Vingtdeux, V., Hamdane, M., Gompel, M., Bégard, S., Drobecq, H., Ghestem, A., Grosjean, M. E., Kostanjevecki, V., Grognet, P., Vanmechelen, E., Buée, L., Delacourte, A., and Sergeant, N. (2005) Phosphorylation of amyloid precursor carboxy-terminal fragments enhances their processing by a gamma-secretase-dependent mechanism. *Neurobiol. Dis.* **20,** 625–637
23. Nakanishi, H. (2003) Neuronal and microglial cathepsins in aging and age-related diseases. *Ageing Res. Rev.* **2,** 367–381
24. Guha, S., and Padh, H. (2008) Cathepsins: fundamental effectors of endolysosomal proteolysis. *Indian J. Biochem. Biophys.* **45,** 75–90
25. Mueller-Steiner, S., Zhou, Y., Arai, H., Roberson, E. D., Sun, B., Chen, J., Wang, X., Yu, G., Esposito, L., Mucke, L., and Gan, L. (2006) Antiamyloidogenic and neuroprotective functions of cathepsin B: implications for Alzheimer's disease. *Neuron* **51,** 703–714
26. Dice, J. F., and Terlecky, S. R. (1990) Targeting of cytosolic proteins to lysosomes for degradation. *Crit. Rev. Ther. Drug Carrier Syst.* **7,** 211–233
27. Cuervo, A. M. (2004) Autophagy: many paths to the same end. *Mol. Cell. Biochem.* **263,** 55–72
28. Kouchi, Z., Sorimachi, H., Suzuki, K., and Ishiura, S. (1999) Proteasome inhibitors induce the association of Alzheimer's amyloid precursor protein with Hsc73. *Biochem. Biophys. Res. Commun.* **254,** 804–810
29. Kinoshita, A., Fukumoto, H., Shah, T., Whelan, C. M., Irizarry, M. C., and Hyman, B. T. (2003) Demonstration by FRET of BACE interaction with the amyloid precursor protein at the cell surface and in early endosomes. *J. Cell Sci.* **116,** 3339–3346
30. Vetrivel, K. S., Cheng, H., Lin, W., Sakurai, T., Li, T., Nukina, N., Wong, P. C., Xu, H., and Thinakaran, G. (2004) Association of γ-secretase with lipid rafts in post-Golgi and endosome membranes. *J. Biol. Chem.* **279,** 44945–44954
31. Thinakaran, G., and Koo, E. H. (2008) Amyloid precursor protein trafficking, processing, and function. *J. Biol. Chem.* **283,** 29615–29619
32. Sun, B., Zhou, Y., Halabisky, B., Lo, I., Cho, S. H., Mueller-Steiner, S., Devidze, N., Wang, X., Grubb, A., and Gan, L. (2008)

Cystatin C-cathepsin B axis regulates amyloid beta levels and associated neuronal deficits in an animal model of Alzheimer's disease. *Neuron* **60,** 247–257
33. Von Rotz, R. C., Kohli, B. M., Bosset, J., Meier, M., Suzuki, T., Nitsch, R. M., and Konietzko, U. (2004) The APP intracellular domain forms nuclear multiprotein complexes and regulates the transcription of its own precursor. *J. Cell Sci.* **117,** 4435–4448
34. Pardossi-Piquard, R., Petit, A., Kawarai, T., Sunyach, C., Alves da Costa, C., Vincent, B., Ring, S., D'Adamio, L., Shen, J., Müller, U., St. George Hyslop, P., and Checler, F. (2005) Presenilin-dependent transcriptional control of the Aβ-degrading enzyme neprilysin by intracellular domains of βAPP and APLP. *Neuron* **46,** 541–554
35. Tagawa, K., Kunishita, T., Maruyama, K., Yoshikawa, K., Kominami, E., Tsuchiya, T., Suzuki, K., Tabira, T., Sugita, H., and Ishiura, S. (1991) Alzheimer's disease amyloid β-clipping enzyme (APP secretase): identification, purification, and characterization of the enzyme. *Biochem. Biophys. Res. Commun.* **177,** 377–387
36. Deussing, J., Roth, W., Saftig, P., Peters, C., Ploegh, H. L., and Villadangos, J. A. (1998) Cathepsins B and D are dispensable for major histocompatibility complex class II-mediated antigen presentation. *Proc. Natl. Acad. Sci. U. S. A.* **95,** 4516–4521
37. Felbor, U., Kessle, B., Mothes, W., Goebel, H. H., Ploegh, H. L., Bronson, R. T., and Olsen, B. R. (2002) Neuronal loss and brain atrophy in mice lacking cathepsins B and L. *Proc. Natl. Acad. Sci. U. S. A.* **99,** 7883–7888
38. Hook, V. Y., Kindy, M., Reinheckel, T., Peters, C., and Hook, G. (2009) Genetic cathepsin B deficiency reduces β-amyloid in transgenic mice expressing human wild-type amyloid precursor protein. *Biochem. Biophys. Res. Commun.* **386,** 284–288
39. Klein, D. M., Felsenstein, K. M., and Brenneman, D. E. (2009) Cathepsins B and L differentially regulate amyloid precursor protein processing. *J. Pharmacol. Exp. Ther.* **328,** 813–821
40. Kim, S. H., and Suh, Y. H. (1996) Neurotoxicity of a carboxyl-terminal fragment of the Alzheimer's amyloid precursor protein. *J. Neurochem.* **67,** 1172–1182
41. Ghosal, K., Vogt, D. L., Liang, M., Shen, Y., Lamb, B. T., and Pimplikar, S. W. (2009) Alzheimer's disease-like pathological features in transgenic mice expressing the APP intracellular domain. *Proc. Natl. Acad. Sci. U. S. A.* **106,** 18367–18372
42. Ando, K., Iijima, K. I., Elliott, J. I., Kirino, Y., and Suzuki, T. (2001) Phosphorylation-dependent regulation of the interaction of amyloid precursor protein with Fe65 affects the production of β-amyloid. *J. Biol. Chem.* **276,** 40353–40361
43. Suzuki, T., and Nakaya, T. (2008) Regulation of amyloid β-protein precursor by phosphorylation and protein interactions. *J. Biol. Chem.* **283,** 29633–29637
44. Rockenstein, E., Torrance, M., Adame, A., Mante, M., Bar-on, P., Rose, J. B., Crews, L., and Masliah, E. (2007) Neuroprotective effects of regulators of the glycogen synthase kinase-3β signaling pathway in a transgenic model of Alzheimer's disease are associated with reduced amyloid precursor protein phosphorylation. *J. Neurosci.* **27,** 1981–1991
45. Citron, M. (2010) Alzheimer's disease: strategies for disease modification. *Nat. Rev. Drug Discov.* **9,** 387–398
46. Janssens, V., and Goris, J. (2001) Protein phosphatase 2A: a highly regulated family of serine/threonine phosphatases implicated in cell growth and signaling. *Biochem. J.* **353,** 417–439
47. Liu, F., Grundke-Iqbal, I., Iqbal, K., and Gong, C. X. (2005) Contributions of protein phosphatases PP1, PP2A, PP2B and PP5 to the regulation of tau phosphorylation. *Eur. J. Neurosci.* **22,** 1942–1950

*Received for publication February 1, 2011.*
*Accepted for publication June 23, 2011.*

Neuroscience Letters 503 (2011) 234–239

Contents lists available at SciVerse ScienceDirect

Neuroscience Letters

journal homepage: www.elsevier.com/locate/neulet

# Protective role of the ubiquitin binding protein Tollip against the toxicity of polyglutamine-expansion proteins

Asami Oguro[a,1], Hiroshi Kubota[b], Miho Shimizu[c], Shoichi Ishiura[a], Yoriko Atomi[d,*]

[a] Department of Life Sciences, The Graduate School of Arts and Sciences, The University of Tokyo, Meguro-ku, Tokyo 153-8902, Japan
[b] Department of Life Science, Faculty and Graduate School of Engineering and Resource Science, Akita University, 1-1 Tegatagakuen-cho, Akita 010-8502, Japan
[c] Graduate School of Information Science and Technology, The University of Tokyo, 7-3-1, Hongo, Bunkyo-ku, Tokyo 113-8656, Japan
[d] The University of Tokyo, Radioisotope Center Cell to Body Dynamics Laboratory 1 2-11-16, Yayoi, Bunkyo-ku, Tokyo 113-0032, Japan

ARTICLE INFO

*Article history:*
Received 7 January 2011
Received in revised form 3 August 2011
Accepted 22 August 2011

*Keywords:*
Aggregation
Huntingtin
Polyglutamine
Tollip

ABSTRACT

Huntington disease (HD) is caused by the expansion of polyglutamine (polyQ) repeats in the amino-terminal of hungtintin (htt). PolyQ-expanded htt forms intracellular ubiquitinated aggregates in neurons and causes neuronal cell death. Here, utilizing a HD cellular model, we report that Tollip, an ubiquitin binding protein that participates in intracellular transport *via* endosomes, co-localizes with and stimulates aggregation of polyQ-expanded amino-terminal htt. Furthermore, we demonstrate that Tollip protects cells against the toxicity of polyQ-expanded htt. We propose that association of Tollip with polyubiquitin accelerates aggregation of toxic htt species into inclusions and thus provides a cell protective role by sequestration.



Huntington disease (HD, OMIM-143100) is a progressive autosomal dominant neurodegenerative disorder caused by expansion of polyglutamine (polyQ) in the hungtintin (htt) protein. The gene encoding htt contains a CAG repeat in exon 1, and this repeat is expanded in HD patients. Although full-length htt is ubiquitously expressed as a 348-kDa cytoplasmic protein, the amino-terminal fragments of polyQ expanded htt ($htt^{PQ}$) tend to form ubiquitinated intracellular aggregates and exert toxicity in neuronal cells [1]. $Htt^{PQ}$ has been shown to cause protein misfolding, aberrant transcription, chaperone activity inhibition and proteasome dysfunction, although the exact molecular mechanism by which polyQ exerts cellular toxicity is unknown [8].

Tollip (Toll-interacting protein) is a ubiquitin binding protein that is involved in sorting of ubiquitinated proteins from endosomes to lysosomes for degradation including that of interleukin-1 receptor (IL-1R) [3,4]. Tollip binds to ubiquitin through the CUE (coupling of ubiquitin to ER degradation) domain and interacts with clathrin and Tom1 (target of Myb protein 1), leading to formation of a multi protein complex for protein degradation [9]. Tollip is localized in endosomes, and disruption of the *Tollip* gene results in accumulation of IL-1R in endosomes and deficiency in lysosomal degradation of IL-1R [3]. Tollip is reported as a protein concentrated in polyglutamine aggregates [5], and the ubiquitin binding protein p62 (also known as sequestosome 1) is known to mediate autophagy-dependent clearance of polyQ aggregates with accelerating $htt^{PQ}$ aggregation [13]. These observations suggested that, like p62, Tollip may be involved in $htt^{PQ}$ aggregation and degradation through ubiquitin binding and membrane sorting activities. Thus, we decided to analyze the role of Tollip in $htt^{PQ}$ aggregation, trafficking and cytotoxicity in neuronal cells.

*Experimental procedures*: The *htt* expression constructs, pIND-tNhtt-EGFP-60Q and pIND-tNhtt-EGFP-150Q, and the generation of the stable Neuro2a cell lines expressing htt proteins were provided by Dr. Nukina [7]. The stable cell lines (HD60Q and HD150Q) were maintained in DMEM supplemented with 10% fetal bovine serum, 0.4 mg/ml Zeocin and 0.4 mg/ml G418 (Sigma). All transfections were performed using the Lipofectamine 2000 reagent (Invitrogen) according to the manufacturer's instructions. To knockdown *Tollip*, cells were transiently transfected with *Tollip* stealth siRNA duplex oligoribonucleotides, 5′-UCUCAAGGUAGAACGAGUCCACACC-3′ and 5′-GGUGUGGACUCGUUCUACCUUGAGA-3′ or Stealth RNAi Negative Control Duplexes, while *Tollip* overexpression was achieved by transiently transfected with the RFP-Tollip expression vector [mouse *Tollip* cloned into the RFPc1 vector (Invitrogen)]. To assess if levels of *Tollip* affected aggregate formation, cells were transiently cotransfected with either GFP-Tollip (or empty GFP cassette) and *htt* (20Q, 80Q or 87Q) exon1 fused with a V5 tag. Twelve hours after transfection, 1 μM of ponasterone A (Invitrogen) for induction of

* Corresponding author. Tel.: +81 3 5841 3055; fax: +81 3 5841 3055.
*E-mail addresses:* oguroasami@ucla.edu (A. Oguro), hkubota@ipc.akita-u.ac.jp (H. Kubota), mshimizu@ynl.t.u-tokyo.ac.jp (M. Shimizu), cishiura@mail.ecc.u-tokyo.ac.jp (S. Ishiura), atomi@bio.c.u-tokyo.ac.jp (Y. Atomi).
[1] Present address: Department of Neurology, David Geffen School of Medicine, University of California, Los Angeles, CA 90095, USA.

0304-3940/$ – see front matter © 2011 Elsevier Ireland Ltd. All rights reserved.
doi:10.1016/j.neulet.2011.08.043

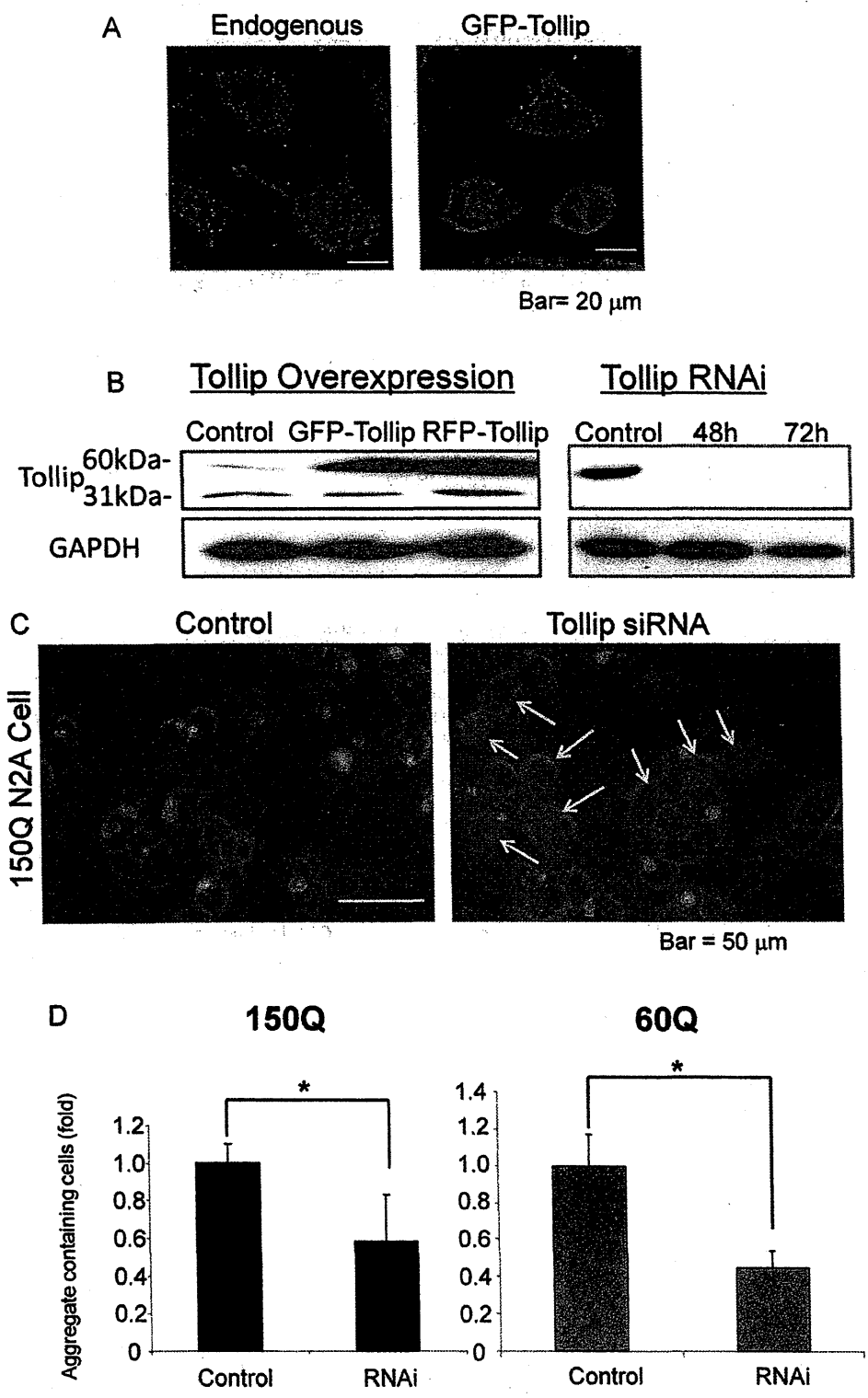


**Fig. 1.** Tollip associates with aggregates of polyQ-expanded htt and affects polyQ aggregation. (A) GFP-Tollip overexpression shows the same localization pattern as endogenous Tollip in the htt150Q Neuro2a cell line without induction. At 48 h of transfection, cells were analyzed by immunostaining. Tollip distributed in small granular particles in the cytoplasm. Bar = 20 μm. (B) Cells were transiently transfected with GFP-*Tollip* or RFP-*Tollip* for 48 h (left), or *Tollip* siRNA for 48–72 h (right). Tollip expression level was analyzed by Western blotting. (C) Htt150Q-expressing cells were transfected with *Tollip* siRNA or control siRNA for 48 h. *Tollip* siRNA treated cells exhibits decreased $htt^{pQ}$ aggregation. Arrows indicate GFP-positive cells that do not form $htt^{pQ}$ aggregates. Bar = 50 μm. (D) *Tollip* knockdown inhibits $htt^{pQ}$ aggregation. HD150Q and HD60Q cells were transfected with *Tollip* siRNA or control siRNA, and aggregate-containing cells were counted ($n = 3$). *, $p < 0.01$.

aggregation was added to the culture and then incubated for an additional 24 h. To count aggregate containing cells, $1 \times 10^3$ cells were seeded into chambered slides, and aggregate containing cells were manually counted using a fluorescence microscope. To test cell death, $5 \times 10^5$ cells were inoculated into each well of 6-well plates, 48 h following transfection, cells were differentiated with 5 mM dibutyryl cyclic AMP in the presence of 1 μM of ponasterone A and allowed to incubate for three days. Aggregate counting experiments were performed after cells were transiently transfected with *Tollip* stealth siRNA duplex or plasmid expression vector (transfection efficiency was almost 90% in Neuro2a cells), and more than 200 cells were counted. Dead cells were counted by propidium iodide staining as described previously [10], and cell viability was measured using Titer Blue assay kit (Promega). Statistical analysis was performed by Student's *t*-test. To inhibit the proteasome, cells were treated with carbobenzoxy-L-leucyl-L-leucyl-L-leucinal (MG-132; Wako, Osaka, Japan) and microtubule destabilization was performed using nocodazole (Sigma).

For immunofluorescence experiments, cells were fixed with 4% paraformaldehyde in PBS for 20 min and blocked with 0.2% BSA in TBST (Tris-Buffered Saline Tween-20) for 1 h. Fixed cells were incubated with antibodies against Tollip (rabbit polyclonal, Ref. [21]), vimentin (mouse monoclonal, Abcam), EEA1 (mouse monoclonal, BD Transduction) or syntaxin-7 (rabbit polyclonal, Abcam) at 1:50 dilution (4 °C, overnight). After several washes with TBST, cells were incubated with Alexa488- or Alexa546-conjigated secondary antibodies (1:2000) for 1 h. After washes, cells were mounted in antifade solution. Immunofluoresent staining of Tollip in HD150Q cells was carried out as described [7]. Solubility of proteins was examined as follows: cells were scraped, homogenized and lysed in PBS supplemented with protease inhibitor cocktail (Sigma) on ice. Cell lysates were briefly sonicated, centrifuged for 10 min at 15,000 × g at 4 °C, and supernatants (soluble fraction) and pellet (insoluble fraction) were analyzed by Western blotting [21].

To examine whether Tollip affects $htt^{pQ}$ aggregation, we established Tollip overexpression and knockdown system *in vitro* (Fig. 1A and B). After overexpression of Tollip using GFP-Tollip construct, transfected Neuro2a cells showed essentially the same localization pattern as endogenous Tollip in cytosol (Fig. 1A), while expression levels of GFP/RFP-Tollip were significantly higher than endogenous Tollip (Fig. 1B, left). Treatment of Neuro2a cells with *Tollip* siRNA diminished endogenous Tollip protein after 48 h through 72 h (Fig. 1B, right). Under the Tollip knockdown conditions, the number of cells that contain htt (150Q and 60Q) aggregates was significantly reduced to approximately 50% (Fig. 1C and D). These results indicate that Tollip stimulates polyQ aggregation in living cells.

Since many polyQ binding proteins affects polyQ-dependent cell death [18], we hypothesized that association of Tollip with $htt^{pQ}$ aggregates may affect polyQ toxicity. Overexpression of Tollip significantly stimulated aggregation of GFP-htt60Q (Fig. 2A), and suppressed cell death in the htt80Q and htt87Q lines (Fig. 2B). In contrast, Tollip overexpression provided no significant difference on the cell death of htt20Q expressing cells (Fig. 2B). Thus, Tollip protects cells against the toxicity of expanded polyQ concomitant with stimulating $htt^{pQ}$ aggregation into aggresomes.

Previous reports indicated that Tollip contains the ubiquitin binding CUE domain [15,20]. Ubiquitin binding motifs are also found in p62 and ubiquilin1, and these proteins function in the ubiquitin–proteasome pathway [6,18]. To investigate whether Tollip distribution is affected by proteasomal inhibition, Neuro2a cells treated with the proteasome inhibitor MG-132 and localization of Tollip was analyzed by immunofluorescence microscopy (Fig. 3A). MG-132 treatment frequently induced formation of juxtanuclear Tollip-containing inclusions surrounded by vimentin, of which specific structure is a marker of the aggresome. We next treated cells

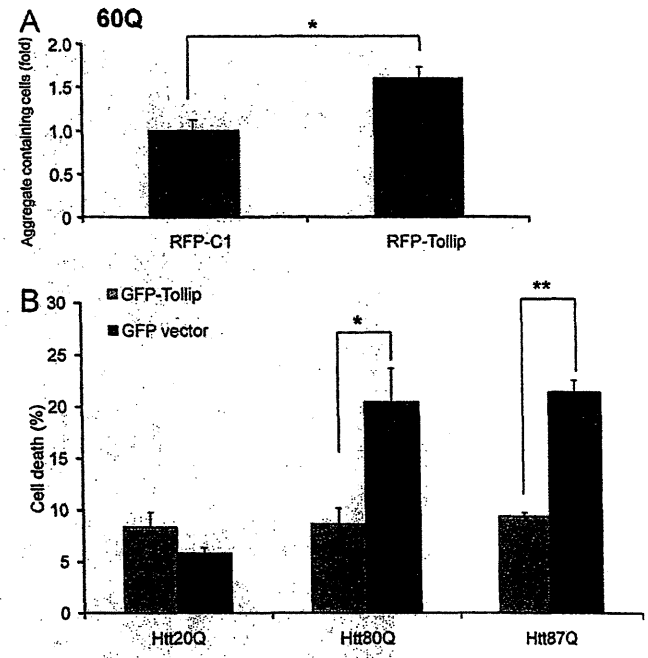


**Fig. 2.** Overexpression of Tollip induces $htt^{pQ}$ aggregation and reduces cell death. (A) Htt-expressing cells were transfected with RFP-Tollip or RFP-C as a control, and aggregate-containing cells were counted ($n = 4$). (B) Tollip protects cells against the toxicity of $htt^{pQ}$. Neuro2a cells were transiently co-transfected with htt (20Q, 80Q or 87Q) and GFP-Tollip (or GFP as a control). Cells were differentiated in the presence of 5 mM dbcAMP. Cell death was analyzed by propidium iodide staining ($n = 4$). More than 300 cells were counted for each experiment. *, $p < 0.01$; **, $p < 0.001$.

with the microtubule-destabilizing drug nocodazole, because formation and maintenance of aggresomes are known to be dependent on microtubule-dependent transport system. Treatment of cells with nocodazole resulted in a more dispersed distribution of Tollip in the cytoplasm in the presence of MG-132. These results indicate that Tollip is concentrated in the aggresome and/or in the region surrounding the aggresome. Centrifugal fractionation indicated that Tollip was present in the insoluble fractions after MG132 treatment (Fig. 3B). Given the insoluble nature of the aggresome, this suggests that Tollip is associated with this structure.

Tollip is known to play a role in endosomal protein trafficking; therefore we performed immunostaining of Tollip with EEA1 (an early endosome marker) or syntaxin-7 (a late endosome marker) in cultured Neuro2a and HEK293 cells after treatment with MG-132 (Fig. 4A). Tollip was rarely found in early endosomes but partly distributed in late endosomes under normal conditions. After MG132 treatment, however, Tollip was highly colocalized with the late endosome marker syntaxin-7. Previous studies indicated that Tollip is known to be accumulated in $htt^{pQ}$ inclusions in the brain of HD model mouse (R6/1) [21]. We thus tested whether Tollip associates with $htt^{pQ}$ aggregates in the HD cellular model [7]. Expression of GFP-htt150Q was induced for 24 h in the presence of ponasterone A, and localization of Tollip was analyzed by immunofluorescence staining. Strong Tollip staining surrounding $htt^{pQ}$ aggregates was observed (Fig. 4B, upper). We also analyzed localization of syntaxin-7 in htt150Q expressing cells and found that syntaxin-7 colocalizes with $htt^{pQ}$ aggregates (Fig. 4B, lower). Thus, Tollip function may be associated with recruitment of misfolded proteins to aggresomes *via* late endosomes, including the case of $htt^{pQ}$. Under MG132-induced stress conditions, overexpression of Tollip significantly protected cells from the toxicity of the proteasome inhibitor (Fig. 4C, left). Furthermore, knockdown of Tollip significantly decreased cell viability of MG132-treated cells (Fig. 4C, right). These results indicate that

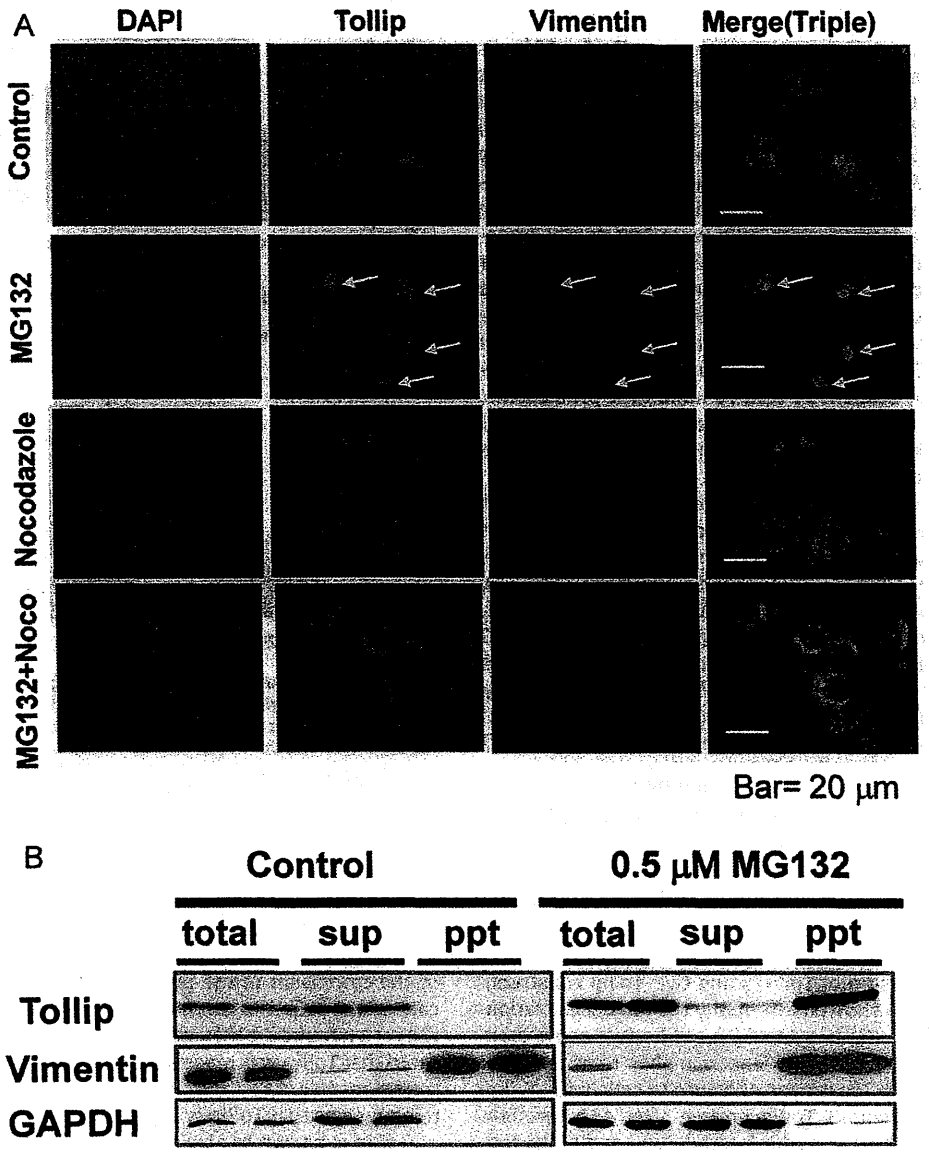


**Fig. 3.** Proteasome inhibition causes accumulation of Tollip in the aggresome. (A) After treatment with 0.5 μM MG-132 for 24 h, cells were stained with antibodies against Tollip and vimentin. Arrows indicate aggresomes surrounded by vimentin cage in Neuro2a cells. Alternatively, after treatment of Neuro2a cells with 10 μM nocodazole and 0.5 μM MG-132 for 12 h, cells were analyzed by immunostaining. Tollip exhibited multiple, small and granular distribution in the cytoplasm after nocodazole treatment. Bar = 20 μm. (B) Western blot analysis of soluble (sup) and insoluble (ppt) fractions prepared from Neuro2a cells after treatment with MG-132 for 24 h or untreated as a control. Blotted proteins were analyzed with indicated antibodies.

Tollip is required for maintaining cell viability against the toxicity of misfolded proteins, probably by recruiting them to aggresomes.

The formation of intracellular ubiquitinated aggregates is a hallmark of polyQ diseases including HD. Transcription factors, molecular chaperones and ubiquitin–proteasome system proteins are known to associate with the polyQ aggregates and implicated in the pathogenesis of polyQ disease [18]. However, role of aggregation in the toxicity is controversial, because accumulating evidence suggests that controlled aggregation into inclusion bodies has cell protective roles against misfolded proteins including polyQ-expanded proteins [16,17]. Tollip is involved in two major cascades of cellular functions. Firstly, Tollip interacts with the TIR domain of the IL-1R [4]. Since the TIR domain mediates the binding of the serine/threonine kinase IRAK-1 to the activated receptor complex, Tollip acts as a regulator of the signaling cascade. Secondly, Tollip is known to interact with polyubiquitinated proteins through the CUE domain and is involved in the ubiquitin–proteasome system. In the case of IL-1R, the CUE domain and TIR interacting domain of Tollip are required for endosome-mediated lysosomal degradation of IL-1R [3]. In the present study, we analyzed the role of Tollip in $htt^{pQ}$ aggregation and cytotoxicity and found that Tollip associates with the $htt^{pQ}$ aggregates and protect cells against $htt^{pQ}$ toxicity by stimulating aggregation (Figs. 1 and 2).

Tollip is a multifunctional protein that interacts with a number of ubiquitin-related proteins and sumolylated proteins, and forms a complex with TOM1, polyubiquitin chains and clathrin heavy chain [9]. As Tollip localizes in endosomes [3], Tollip can function as a molecular link between endosomal processing and ubiquitin–proteasome system. In the present study, we demonstrate that Tollip colocalizes with a late endosome marker in $htt^{pQ}$ aggregates and the aggresome formed under proteasome inhibition

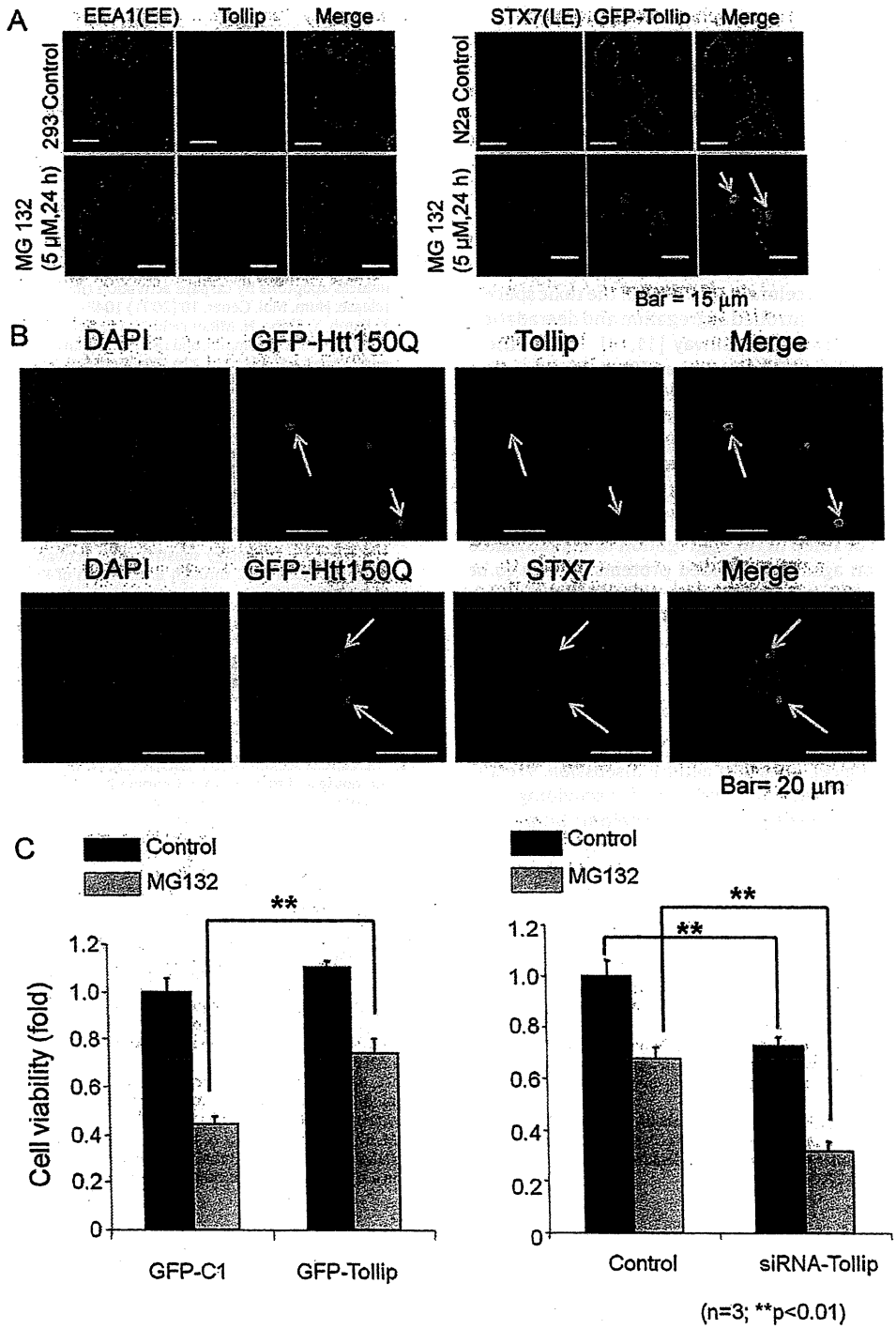


**Fig. 4.** Colocalization of Tollip with a late endosomal maker in MG132-induced aggresomes and $htt^{pQ}$ inclusions and Tollip-dependent cell protection against the toxicity of proteasome inhibition. (A) HEK293 cells were co-stained with antibodies against EEA1 (early endosome marker) and Tollip (left), or GFP-Tollip transfected Neuro2a cells were stained with antibody against syntaxin-7 (late endosome marker) (right). Arrows indicate the co-localization of Tollip with syntaxin-7. Bar = 15 μm. (B) A Neuro2a cell line stably expressing GFP-htt150Q was stained with anti-Tollip (upper) or anti-syntaxin-7 (lower) antibodies. Arrows indicate the co-localization of Tollip and syntaxin-7 in htt aggregates. Bar = 20 μm. (C) After the treatment with 5 μM MG-132 for 24 h, Neuro2a cells were transiently transfected with GFP-Tollip or GFP vector as a control (left). Alternatively, cells were treated with *Tollip* siRNA or control siRNA as a control (right). Cells were then differentiated in the presence of 5 mM dbcAMP. Cell viability was measured by Titer Blue assay (Promega) ($n = 3$). **, $p < 0.001$. The difference of control cell viability between left and right panels is considered to be due to the difference in toxic effect between plasmid DNA transfection and small RNA transfection [11].

conditions (Figs. 3 and 4). These observations strongly suggest that Tollip mediates trafficking of ubiquitinated aberrant proteins to aggresomes *via* late endosomes or structures containing endosomal proteins.

Accumulating evidence indicates that ubiquitin binding proteins play crucial roles in degradation of polyQ proteins through ubiquitin and autophagy systems. For example, the ubiquitin binding protein p62 co-localizes with many types of polyubiquitinated

protein aggregates and recruit the autophagosomal protein LC3 [2]. The p62 protein recognizes polyubiquitin by the carboxyl-terminal UBA domain and is polymerized through the amino-terminal PB1 domain. Expression of p62 is strongly induced by exposure to proteasomal inhibitors or overexpression of polyglutamine-expanded proteins [18], and this protein is required for autophagic clearance of misfolded proteins [2,11,12]. Ubiquilin, another ubiquitin binding protein, protects cells against the toxicity of htt exon-1 (74Q) through authophagy [19]. Formation of inclusions/aggresomes is considered to reduce toxic misfolded species like oligomers, and ubiquitin interacting proteins may stimulate formation of aggresomes to accelerate clearance of the toxic species by microtubule-dependent controlled aggregation and degradation through the autophagy–lysosome pathway [11,14]. These observations suggest that Tollip protects cells perhaps by enhancing controlled aggregation to the aggresome using the ubiquitin binding CUE domain and the ability to interact with multiple proteins (e.g., clathrin and Tom1). Since Tollip is involved in protein transport *via* endosomes [9] and Tollip colocalized with an endosome maker in aggresomes/inclusions in our experiments, Tollip may accerelate aggregation of ubiquitinated proteins *via* endosomes, although precise roles of Tollip in the aggregation of ubiquitinated proteins and protection against misfolded proteins remain to be investigated. In conclusion, our present data indicate that Tollip is a cell protective ubiquitin binding protein that stimulates aggresome/inclusion formation in neuronal cells.

## Acknowledgements

We thank Dr. Nobuyuki Nukina (RIKEN Brain Institute) for kindly providing htt expressing cell lines and helpful discussion. We also thank Drs. Takashi Tsuboi (University of Tokyo) for providing helpful ideas, Kouta Kanno (University of Tokyo) for helping htt plasmid preparation and Brent Bill (UCLA) for giving helpful advice. AO was supported by a fellowship from Japan Society for Promotion of Science.

## References

[1] The Huntington's Disease Collaborative Research Group, A novel gene containing a trinucleotide repeat that is expanded and unstable on Huntington's disease chromosomes, Cell 72 (1993) 971–983.
[2] G. Bjorkoy, T. Lamark, A. Brech, H. Outzen, M. Perander, A. Overvatn, H. Stenmark, T. Johansen, p62/SQSTM1 forms protein aggregates degraded by autophagy and has a protective effect on huntingtin-induced cell death, J. Cell Biol. 171 (2005) 603–614.
[3] B. Brissoni, L. Agostini, M. Kropf, F. Martinon, V. Swoboda, S. Lippens, H. Everett, N. Aebi, S. Janssens, E. Meylan, M. Felberbaum-Corti, H. Hirling, J. Gruenberg, J. Tschopp, K. Burns, Intracellular trafficking of interleukin-1 receptor I requires Tollip, Curr. Biol. 16 (2006) 2265–2270.
[4] K. Burns, J. Clatworthy, L. Martin, F. Martinon, C. Plumpton, B. Maschera, A. Lewis, K. Ray, J. Tschopp, F. Volpe, Tollip a new component of the IL-1RI pathway, links IRAK to the IL-1 receptor, Nat. Cell Biol. 2 (2000) 346–351.
[5] H. Doi, K. Mitsui, M. Kurosawa, Y. Machida, Y. Kuroiwa, N. Nukina, Identification of ubiquitin-interacting proteins in purified polyglutamine aggregates, FEBS Lett. 571 (2004) 171–176.
[6] R. Heir, C. Ablasou, E. Dumontier, M. Elliott, C. Fagotto-Kaufmann, F.K. Bedford, The UBL domain of PLIC-1 regulates aggresome formation, EMBO Rep. 7 (2006) 1252–1258.
[7] N.R. Jana, N. Nukina, BAG-1 associates with the polyglutamine-expanded huntingtin aggregates, Neurosci. Lett. 378 (2005) 171–175.
[8] N.R. Jana, E.A. Zemskov, G. Wang, N. Nukina, Altered proteasomal function due to the expression of polyglutamine-expanded truncated N-terminal huntingtin induces apoptosis by caspase activation through mitochondrial cytochrome c release, Hum. Mol. Genet. 10 (2001) 1049–1059.
[9] Y. Katoh, Y. Shiba, H. Mitsuhashi, Y. Yanagida, H. Takatsu, K. Nakayama, Tollip and Tom1 form a complex and recruit ubiquitin-conjugated proteins onto early endosomes, J. Biol. Chem. 279 (2004) 24435–24443.
[10] A. Kitamura, H. Kubota, C.G. Pack, G. Matsumoto, S. Hirayama, Y. Takahashi, H. Kimura, M. Kinjo, R.I. Morimoto, K. Nagata, Cytosolic chaperonin prevents polyglutamine toxicity with altering the aggregation state, Nat. Cell Biol. 8 (2006) 1163–1170.
[11] M. Komatsu, Y. Ichimura, Physiological significance of selective degradation of p62 by autophagy, FEBS Lett. 584 (2010) 1374–1378.
[12] M. Komatsu, H. Kurokawa, S. Waguri, K. Taguchi, A. Kobayashi, Y. Ichimura, Y.S. Sou, I. Ueno, A. Sakamoto, K.I. Tong, M. Kim, Y. Nishito, S. Iemura, T. Natsume, T. Ueno, E. Kominami, H. Motohashi, K. Tanaka, M. Yamamoto, The selective autophagy substrate p62 activates the stress responsive transcription factor Nrf2 through inactivation of Keap1, Nat. Cell Biol. 12 (2010) 213–223.
[13] M. Komatsu, S. Waguri, M. Koike, Y.S. Sou, T. Ueno, T. Hara, N. Mizushima, J. Iwata, J. Ezaki, S. Murata, J. Hamazaki, Y. Nishito, S. Iemura, T. Natsume, T. Yanagawa, J. Uwayama, E. Warabi, H. Yoshida, T. Ishii, A. Kobayashi, M. Yamamoto, Z. Yue, Y. Uchiyama, E. Kominami, K. Tanaka, Homeostatic levels of p62 control cytoplasmic inclusion body formation in autophagy-deficient mice, Cell 131 (2007) 1149–1163.
[14] R.R. Kopito, Aggresomes, inclusion bodies and protein aggregation, Trends Cell Biol. 10 (2000) 524–530.
[15] Y.L. Lo, A.G. Beckhouse, S.L. Boulus, C.A. Wells, Diversification of TOLLIP isoforms in mouse and man, Mamm. Genome 20 (2009) 305–314.
[16] R. Luthi-Carter, D.M. Taylor, J. Pallos, E. Lambert, A. Amore, A. Parker, H. Moffitt, D.L. Smith, H. Runne, O. Gokce, A. Kuhn, Z. Xiang, M.M. Maxwell, S.A. Reeves, G.P. Bates, C. Neri, L.M. Thompson, J.L. Marsh, A.G. Kazantsev, SIRT2 inhibition achieves neuroprotection by decreasing sterol biosynthesis, Proc. Natl. Acad. Sci. U.S.A. 107 (2010) 7927–7932.
[17] R.I. Morimoto, Proteotoxic stress and inducible chaperone networks in neurodegenerative disease and aging, Genes Dev. 22 (2008) 1427–1438.
[18] U. Nagaoka, K. Kim, N.R. Jana, H. Doi, M. Maruyama, K. Mitsui, F. Oyama, N. Nukina, Increased expression of p62 in expanded polyglutamine-expressing cells and its association with polyglutamine inclusions, J. Neurochem. 91 (2004) 57–68.
[19] C. Rothenberg, D. Srinivasan, L. Mah, S. Kaushik, C.M. Peterhoff, J. Ugolino, S. Fang, A.M. Cuervo, R.A. Nixon, M.J. Monteiro, Ubiquilin functions in autophagy and is degraded by chaperone-mediated autophagy, Hum. Mol. Genet. 19 (2010) 3219–3232.
[20] S.C. Shih, G. Prag, S.A. Francis, M.A. Sutanto, J.H. Hurley, L. Hicke, A ubiquitin-binding motif required for intramolecular monoubiquitylation, the CUE domain, EMBO J. 22 (2003) 1273–1281.
[21] M. Tanaka, Y. Machida, S. Niu, T. Ikeda, N.R. Jana, H. Doi, M. Kurosawa, M. Nekooki, N. Nukina, Trehalose alleviates polyglutamine-mediated pathology in a mouse model of Huntington disease, Nat. Med. 10 (2004) 148–154.

# RNA結合蛋白質が引き起こす筋強直性ジストロフィー

Myotonic dystrophy and RNA-binding proteins

古戎道典(写真)　石浦章一
Michinori Koebisu and Shoichi Ishiura
東京大学大学院総合文化研究科生命環境科学系

◎筋強直性ジストロフィー(DM1)は，CTGリピートの伸長により発症する優性遺伝疾患である．伸長したリピートはさまざまな経路で症状をもたらすが，そのひとつにRNAレベルでの毒性があげられる．これまでの研究で，CUGリピートをもつRNAは複数のRNA結合蛋白質の挙動を変化させ，多様なRNA代謝経路に異常をもたらすことが明らかになってきた．本稿では，そのなかでCELFファミリーとMBNLファミリーという2つのRNA結合蛋白質に焦点を絞り，DM1の病理機構のなかでどのような役割を担っているかについて概観したい．

Key word：筋強直性ジストロフィー(DM1)，選択的スプライシング，翻訳制御，mRNA分解

## DM1の発症機構

筋強直性ジストロフィー(myotonic dystrophy type 1：DM1)で異常伸長がみられるCTGリピートは，DMPK遺伝子の3'非翻訳領域(3'UTR)に存在する[1-4]．そのためCTGリピートの伸長は蛋白質のアミノ酸配列には直接影響しないが，伸長したリピートはその周辺のヘテロクロマチン構造を変化させたり[5,6]，DMPK遺伝子の転写産物の核外搬出を阻害したりして[7]，DMPK遺伝子やその下流にあるSIX5遺伝子の発現量を抑制すると考えられている[8,9]．ノックアウトマウスの解析から，これらの遺伝子の発現量の低下が一部の症状を引き起こすことが示唆されており，伸長リピートによる遺伝子発現の抑制は，DM1の病理機構の重要な側面となっている[10-12]．一方で，多くの研究が伸長したCTGリピートがRNAレベルで毒性をもつことを示唆している．たとえば，CUGリピートRNAを発現するトランスジェニックマウス($HSA^{LR}$)は，ミオトニアや骨格筋の組織学的な特徴，選択的スプライシングの異常など，DM1患者にみられる症状を再現する[13,14]．*In situ* hybridizationでDM1患者細胞のリピートRNAを検出するとCUGリピートが核内で凝集体を形成することが示され，このCUGリピートの奇妙な挙動も注目を集めてきた[7,15]．

さらに2001年には，DM1とは異なる遺伝子座にリピートの伸長をもつDMの家系がみつかった[16]．この家系では，第3番染色体のZNF9遺伝子のエクソン1に存在するCCTGリピートが伸長している．ZNF9遺伝子やその周辺に遺伝子座をもつ遺伝子は，DMPK遺伝子やSIX5遺伝子との明らかな関連はなく，このあらたなDMの発見は伸長したリピートRNAそれ自体がDMの発症原因になることを強く示唆している．

伸長したCUGリピートRNAは，RNA結合蛋白質の挙動を変化させることで毒性を発揮すると考えられている[17]．すなわち，RNA結合蛋白質がDM1の病理機構の中心的役割を担っているともいえる．CUGリピートRNAに結合する蛋白質として，mucleblind-like(MBNL)とCUG-BP-ETR-3-like factors(CELF)とよばれるRNA結合蛋白質ファミリーが見出され，DM1の症状の発現にこれら2つの蛋白質ファミリーが重要な役割を担うことが，多数の報告で示されている(図1)．DM1で異常となるスプライシングの多くが，これらの蛋白質によって制御されうる．

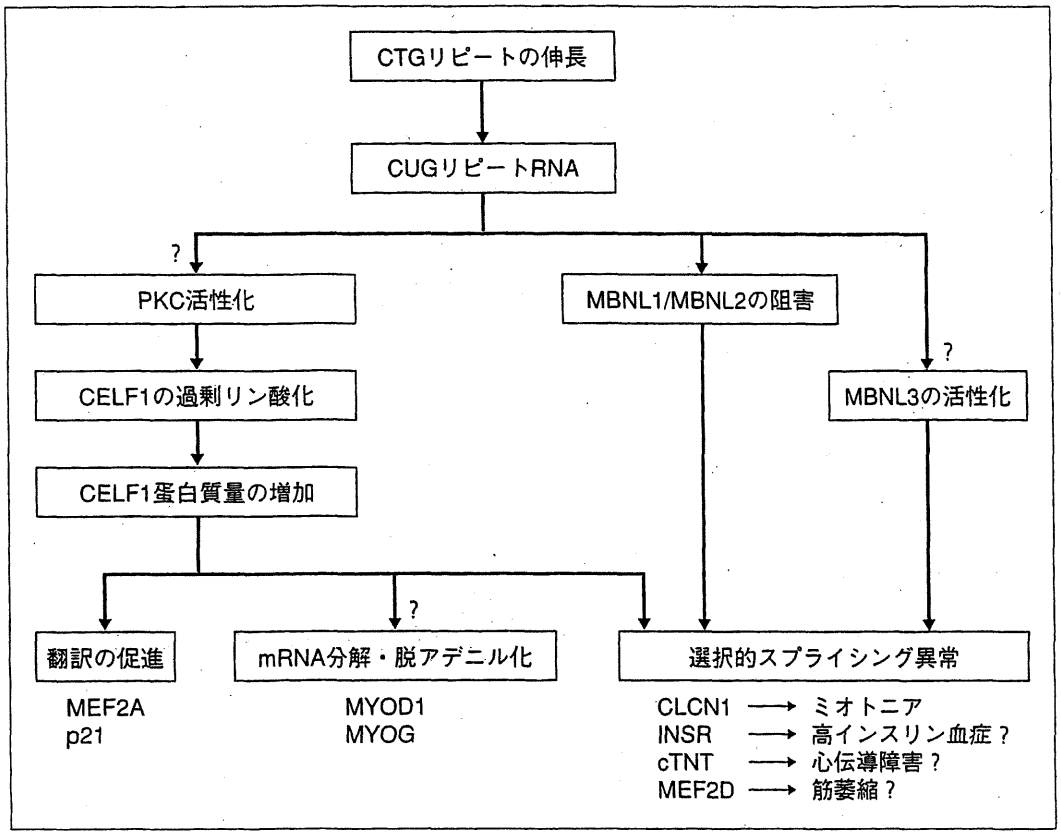


**図 1　DMの発症機構モデル**

本稿ではMBNL，CELFファミリーがそれぞれどのようにDM1の発症に関与しているかについて，最近の報告を踏まえて紹介したい．

## CELF1はリン酸化によって発現量が増加する

CELFファミリーはCELF1/CUG-BP(CUG-binding protein)とCELF2/ETR-3(embryonic lethal abnormal vision type RNA-binding protein 3)のホモログからなるRNA結合蛋白質ファミリーであり，ヒトでは6つのホモログ(CELF1～CELF6)が同定されている．

CELF1はCUG-BPという別名が示すとおり，CUGリピートに結合する蛋白質として発見された[18]．HeLa細胞の抽出物のなかに$(CUG)_8$プローブに結合する蛋白質が見出され，CUG-BPと名づけられたのである．しかしその後の研究で，CELF1はかならずしもCUGリピートに特異的に結合するのではないことが明らかになってきた．たとえば，当研究室の酵母3ハイブリッド法を用いた研究では，CELF1はCUGリピートよりもむしろUGリピートに選択的に結合することが示されている[19]．そうした経緯をもつものの，CELF1はDM1の病理機構のなかで主要な因子として注目され続けている．その理由のひとつは，DM1患者の筋組織でCELF1蛋白質の発現量が上昇していることが観察されることである[20-22]．Kuyumcu-Martinezらは，DM1の細胞でCELF1蛋白質が過剰にリン酸化され分解されにくくなった結果，発現量が上昇していることを示した[23]．また，培養細胞にCUGリピートを発現させるとPKCがリン酸化により活性化し，PKC阻害剤はCELF1リン酸化を阻害した．しかし，リピートRNAがどのようにPKCを活性化するのか，その経路については明らかになっていない．

CELF1が注目されるもうひとつの理由は，CELF1の過剰発現によってDM1でみられる異常のいくつかが再現されることである．たとえば，マウスにCELF1を過剰発現すると中心核や筋変性などの筋障害や心伝導障害を呈することから，CELF1の発現量の上昇は骨格筋や心筋の筋障害に関与しているらしい[24-27]

## CELF1の活性化とDM1の発症

CELF1の発現量の上昇が筋障害をもたらす分子メカニズムについては，明確なことはわかっていない．ひとつの可能性は，筋組織の形成・維持にかかわる選択的スプライシングの異常であるが，近年，CELF1が選択的スプライシングの制御だけでなく，さまざまなRNA代謝や翻訳の制御にも関与することが明らかになってきた．

CELF1はmRNAの脱アデニル化と分解を制御するツメガエルEDEN-BP遺伝子のオルソログであり，EDEN-BP同様にmRNA寿命を制御しているらしい．Moraesらは，CELF1が寿命の短いmRNAに結合し，脱アデニル化を促進することを示した[28]．またVlasovaらは，CELF1がc-junやjunBなどの寿命の短いmRNAに結合しmRNAの分解を抑制すると報告している[29]．さらにLeeらは，RNA免疫沈降法とDNAマイクロアレイを組み合わせた方法(RNA-Chip法)でCELF1によるmRNA分解のターゲットを探索し，Myod1やMyogなどの筋特異的転写調節因子がCELF1のターゲット候補であることを同定した[30]．

一方で，CELF1は翻訳の制御にも関与することが報告されている．Timchenkoらは，CELF1を過剰発現するトランスジェニックマウスの骨格筋でp21とMef2Aの発現量が増加していることを見出した[24]．CELF1はどちらの遺伝子のmRNAにも直接結合し，結合依存的に翻訳を促進する．p21とMEF2Aはどちらも筋分化を促進する作用をもつと考えられており，これらの発現量の上昇はDM1の骨格筋でも観察されることから，DM1の発症機構を考えるにあたってとりわけ興味深い．

## MBNLファミリーはCUGリピートの機能阻害を受ける

一方，MBNLファミリーはショウジョウバエのmuscleblind遺伝子のオルソログであり，muscleblind-likeからこの名がついた．線虫からヒトに至るまで広く保存された遺伝子であり，ヒトやマウスでは3つのアイソフォーム(MBNL1, MBNL2, MBNL3)が同定されている．MBNLもCELFと同様に，CUGリピートに結合する蛋白質としてみつかってきた[31]．CELF1と異なり，MBNL1はCUGリピートおよびCCUGリピートと高い親和性をもち[32]，興味深いことに，DM1の骨格筋切片やCUGリピートを発現させた培養細胞をMBNL抗体で染色すると，MBNL1およびMBNL2がCUGリピートを形成する凝集体と共局在する像が観察される[31,33]．このことから，DM1患者の細胞内ではMBNLファミリー蛋白質がCUGリピートにトラップされ，本来の基質と結合できなくなることで機能が阻害されているのではないかと考えられるようになった．

MBNLの機能阻害がDM1の病理に関与するという仮説は，*Mbnl1*のノックアウトマウスの作製によって広く信じられるようになった[34]．Mbnl1を欠損する$Mbnl1^{\Delta E3/\Delta E3}$マウスは，塩素チャネル*Clcn1*の選択的スプライシングの異常や，ミオトニア，筋線維の中心核，白内障，認知障害など，DM1患者が呈する異常を再現するのである．とくにDM1患者でみられる選択的スプライシング異常に対して，MBNL1の機能低下が重要な役割を担っているらしい．Duらは最近，DNAマイクロアレイを用いて$HSA^{LR}$マウスと$Mbnl1^{\Delta E3/\Delta E3}$マウスのスプライシングパターンを網羅的に探索し，この2系統のマウスが示すスプライシング異常が83%一致するという結果を得ている[14]．またKanadiaらは，CUGリピートを発現する$HSA^{LR}$マウスにMbnl1を過剰発現することで複数の選択的スプライシング異常が改善することを明らかにした[35]．これらの結果は，すくなくとも$HSA^{LR}$マウスの選択的スプライシング異常のかなりの部分が，Mbnl1の機能低下だけで説明できることを示している．

一方で，$Mbnl1^{\Delta E3/\Delta E3}$マウスは筋組織の障害をほとんど示さない．そのひとつの理由は，Mbnl2がMbnl1の欠損を補償しているからかもしれない．実際，*Mbnl2*のノックアウトマウスも選択的スプライシングの異常や筋線維の中心核など，DM1の特徴を再現すると報告されており[36]，DM1患者や$HSA^{LR}$マウスではMBNL1とMBNL2がともにCUGリピートの凝集体にトラップされることで，より重篤な表現型が現れている可能性がある．

MBNL3に関しては最近，患者の骨格筋と心筋

で発現量が増加していることが見出された[37]. MBNL3は，培養細胞にCUGリピートを発現させても発現量の上昇を示す．さらに，MBNL3をマウス筋芽細胞であるC2C12に発現させるとMef2Dの選択的スプライシングの制御を介して筋分化を抑制することも示された．DM1患者におけるMBNL3の発現量上昇のメカニズムや症状への寄与の解明は今後の課題であるが，MBNL1やMBNL2とは異なる機構でDM1病理機構に関与する可能性が示されたのは興味深い．

## RNA結合蛋白質のバランスの異常とDM1

CELF蛋白質とMBNL蛋白質は，Clcn1や心筋トロポニンT遺伝子，インスリン受容体遺伝子などいくつかの選択的スプライシング制御において拮抗的に作用することがわかっている[20,38-40]．また，マウスの心臓では出生後にCELF1の発現量が低下する一方，MBNL1の発現量が増加することから，これらのRNA結合蛋白質の発現量のバランスが筋の成熟を決定するというモデルも提唱されている[41]．しかし，著者らはこれらに反する例も経験しており[42,43]，かならずしも拮抗説が正しいとは言い切れない．DM1においては，CELFとMBNLのバランスの崩れが病理機構の根幹をなしている．これまでみてきたように，とくにCELF1ではさまざまなRNA制御機構を介してDM1の諸症状を引き起こしている可能性があり，DM1の多様な症状がどのような過程で生じるのか，今後さらなる解明が期待される．

### 文献


1) Brook, J. D. et al. : *Cell*, **68** : 799-808, 1992.
2) Aslanidis, C. et al. : *Nature*, **355** : 548-551, 1992.
3) Buxton, J. et al. : *Nature*, **355** : 547-548, 1992.
4) Harley, H. G. et al. : *Nature*, **355** : 545-546, 1992.
5) Steinbach, P. et al. : *Am. J. Hum. Genet.*, **62** : 278-285, 1998.
6) Otten, A. D. and Tapscott, S. J. : *Proc. Natl. Acad. Sci. USA*, **92** : 5465-5469, 1995.
7) Davis, B. M. et al. : *Proc. Natl. Acad. Sci. USA*, **94** : 7388-7393, 1997.
8) Thornton, C. A. et al. : *Nat. Genet.*, **16** : 407-409, 1997.
9) Boucher, C. A. et al. : *Hum. Mol. Genet.*, **4** : 1919-1925, 1995.
10) Reddy, S. et al. : *Nat. Genet.*, **13** : 325-335, 1996.
11) Sarkar, P. S. et al. : *Nat. Genet.*, **25** : 110-114, 2000.
12) Klesert, T. R. et al. : *Nat. Genet.*, **25** : 105-109, 2000.
13) Mankodi, A. et al. : *Science*, **289** : 1769-1773, 2000.
14) Du, H. et al. : *Nat. Struct. Mol. Biol.*, **17** : 187-193, 2010.
15) Taneja, K. L. et al. : *J. Cell Biol.*, **128** : 995-1002, 1995.
16) Liquori, C. L. et al. : *Science*, **293** : 864-867, 2001.
17) Ranum, L. P. and Cooper, T. A. : *Annu. Rev. Neurosci.*, **29** : 259-277, 2006.
18) Timchenko, L. T. et al. : *Nucleic Acids Res.*, **24** : 4407-4414, 1996.
19) Takahashi, N. et al. : *Biochem. Biophys. Res. Commun.*, **277** : 518-523, 2000.
20) Savkur, R. S. et al. : *Nat. Genet.*, **29** : 40-47, 2001.
21) Timchenko, N. A. et al. : *Mol. Cell. Biol.*, **21** : 6927-6238, 2001.
22) Ladd, A. N. et al. : *J. Biol. Chem.*, **279** : 17756-17764, 2004.
23) Kuyumcu-Martinez, N. M. et al. : *Mol. Cell*, **28** : 68-78, 2007.
24) Timchenko, N. A. et al. : *J. Biol. Chem.*, **279** : 13129-13139, 2004.
25) Ho, T. H. et al. : *Hum. Mol. Genet.*, **14** : 1539-1547, 2005.
26) Koshelev, M. et al. : *Hum. Mol. Genet.*, **19** : 1066-1075, 2010.
27) Ward, A. J. et al. : *Hum. Mol. Genet.*, **19** : 3614-3622, 2010.
28) Moraes, K. C. et al. : *RNA*, **12** : 1084-1091, 2006.
29) Vlasova, I. A. et al. : *Mol. Cell*, **29** : 263-270, 2008.
30) Lee, J. E. et al. : *PLoS One*, **5** : e11201, 2010.
31) Miller, J. W. et al. : *EMBO J.*, **19** : 4439-4448, 2000.
32) Kino, Y. et al. : *Hum. Mol. Genet.*, **13** : 495-507, 2004.
33) Fardaei, M. et al. : *Nucleic Acids Res.*, **29** : 2766-2771, 2001.
34) Kanadia, R. N. et al. : *Science*, **302** : 1978-1980, 2003.
35) Kanadia, R. N. et al. : *Proc. Natl. Acad. Sci. USA*, **103** : 11748-11753, 2006.
36) Hao, M. et al. : *Dev. Dyn.*, **237** : 403-410, 2008.
37) Lee, K. S. et al. : *J. Biol. Chem.*, **285** : 33779-33787, 2010.
38) Kino, Y. et al. : *Nucleic Acids Res.*, **37** : 6477-6490, 2009.
39) Philips, A. V. et al. : *Science*, **280** : 737-741, 1998.
40) Ho, T. H. et al. : *EMBO J.*, **23** : 3103-3112, 2004.
41) Kalsotra, A. et al. : *Proc. Natl. Acad. Sci. USA*, **105** : 20333-20338, 2008.
42) Koebis, M. et al. : *Genes Cells*, 2011. (in press)
43) Ohsawa, M. et al. : *Biochem. Biophys. Res. Commum.*, **409** : 64-69, 2011.

Journal of Neuroscience Research

Journal of Neuroscience Research 90:870–877 (2012)

# Localization of Mature Neprilysin in Lipid Rafts

**Kimihiko Sato,[1] Chiaki Tanabe,[2] Yoji Yonemura,[1] Haruhiko Watahiki,[1] Yimeng Zhao,[1] Sosuke Yagishita,[1] Maiko Ebina,[1] Satoshi Suo,[1] Eugene Futai,[1] Masayuki Murata,[1] and Shoichi Ishiura[1]***

[1]Department of Life Sciences, Graduate School of Arts and Sciences, The University of Tokyo, Tokyo, Japan

[2]Department of Neuroscience, School of Pharmacy, Iwate Medical University, Morioka, Japan

Alzheimer's disease (AD) is characterized by senile plaques caused by amyloid-β peptide (Aβ) accumulation. It has been reported that Aβ generation and accumulation occur in membrane microdomains, called *lipid rafts*, which are enriched in cholesterol and glycosphingolipids. Moreover, the ablation of cholesterol metabolism has been implicated in AD. Neprilysin (NEP), a neutral endopeptidase, is one of the major Aβ-degrading enzymes in the brain. Activation of NEP is a possible therapeutic target. However, it remains unknown whether the activity of NEP is regulated by its association with lipid rafts. Here we show that only the mature form of NEP, which has been glycosylated in the Golgi, exists in lipid rafts, where it is directly associated with phosphatidylserine. Moreover, the localization of NEP in lipid rafts is enhanced by its dimerization, as shown using the NEP E403C homodimerization mutant. However, the protease activities of the mature form of NEP, as assessed by in vitro peptide hydrolysis, did not differ between lipid rafts and nonlipid rafts. We conclude that cholesterol and other lipids regulate the localization of mature NEP to lipid rafts, where the substrate Aβ accumulates but does not modulate the protease activity of NEP. 

**Key words:** Alzheimer's disease; neprilysin; lipid rafts

Alzheimer's disease (AD) is characterized by the formation of senile plaques, composed primarily of amyloid-β peptide (Aβ). Aβ deposition has been thought to cause neurofibrillary tangles, neuronal cell loss, vascular damage, and dementia (the amyloid hypothesis; Hardy and Higgins, 1992). It has recently been suggested that AD begins with hippocampal synaptic dysfunction caused by diffusible oligomeric assemblies of Aβ (Selkoe, 2002).

Aβ is produced from amyloid precursor protein (APP) by the action of β- and γ-secretases, although APP is usually cleaved within the Aβ sequence by α-secretase. Aβ is degraded by neprilysin (NEP; Iwata et al., 2001). NEP is a type II membrane metallopeptidase that is capable of degrading not only monomeric Aβ but also pathological oligomeric Aβ (Kanemitsu et al., 2003). It has been reported that NEP levels in the hippocampus and cortex decline with age (Iwata et al., 2002; Hellstrom-Lindahl et al., 2008). Thus, analysis of the mechanisms regulating NEP activity may provide valuable insights for new therapeutic targets.

Recently, there have been several reports on the activities of proteases being regulated by their localization to membrane microdomains, known as *lipid rafts*. Lipid rafts, which are enriched in cholesterol and glycosphingolipids, have been implicated in processes such as signal transduction, endocytosis, and cholesterol trafficking (Pike, 2004, 2006). Whereas α-secretase cleavage occurs in nonlipid rafts (Kojro et al., 2001; von Tresckow et al., 2004), Aβ generation occurs in lipid rafts (Wada et al., 2003). It has been reported that Aβ accumulation is initiated by its association with GM1 in lipid rafts (Matsuzaki et al., 2007) and that NEP is partially localized in lipid rafts (Angelisova et al., 1999; Riemann et al., 2001; Kawarabayashi et al., 2004). However, whether the activity of NEP is regulated by its localization in lipid rafts is unknown.

Here we show that localization of glycosylated mature NEP in lipid rafts is regulated by its association with cholesterol. Moreover, we show with the NEP E403C homodimerization mutant that this localization is enhanced by its dimerization. Furthermore, we investigated the protease activities of mature NEP by an in vitro peptide assay. Unexpectedly, they were comparable in lipid rafts and nonlipid rafts. These findings suggest

Additional Supporting Information may be found in the online version of this article.

K. Sato and C. Tanabe contributed equally to this work.

Contract grant sponsor: Ministry of Education, Science, Sports, Culture, and Technology of Japan.

*Correspondence to: Shoichi Ishiura, Department of Life Sciences, Graduate School of Arts and Sciences, The University of Tokyo, 3-8-1 Komaba, Meguro-ku, Tokyo 153-8902, Japan.
E-mail: cishiura@mail.ecc.u-tokyo.ac.jp

Received 2 June 2011; Revised 17 August 2011; Accepted 24 August 2011

**Published online 20 December 2011 in Wiley Online Library (wileyonlinelibrary.com). DOI: 10.1002/jnr.22796**

that cholesterol regulates the localization of mature NEP in lipid rafts, where the substrate Aβ accumulates but apparently does not modulate the protease activity of NEP.

## MATERIALS AND METHODS

### Vectors and Constructs

Human neprilysin, NEP WT, was inserted into the pcDNA3.1-3 × FLAG vector (Invitrogen, Carlsbad, CA), thereby fusing triplet tandem repeats of FLAG tag to its N-terminus. The expression product of this construct will be referred to as FLAG-NEP WT. NEP E584V, carrying a catalytically inactive mutant E584V, and NEP E403C, carrying a homodimerization mutant, were subcloned into the pcDNA3.1-3 × FLAG vector, yielding FLAG-NEP E584V and FLAG-NEP E403C, respectively.

### Antibodies

The following antibodies were purchased: anti-FLAG M2 (Sigma, St. Louis, MO); antiflotillin-1 and anticalnexin (BD Transduction Laboratories, Lexington, KY); anti-monoclonal NEP (Leica Microsystems); and HRP-conjugated anti-mouse IgG (Cell Signaling Technology, Beverly, MA).

### Cell Culture and Transfection

HEK293 cells were cultured in DMEM (Sigma) supplemented with 10% fetal bovine serum (Sigma). They were maintained at 37°C in an atmosphere containing 5% $CO_2$ in a tissue culture incubator. DNA transfection was performed by lipofection with FuGENE 6 Transfection Reagent (Roche, Indianapolis, IN) when cells were 50% confluent. Then, 24 hr later, cells were harvested or used in assays.

### Isolation of the Membrane Fraction

Cells were dissolved in TBS (0.1 M Tris-HCl, pH 8.0, 150 mM NaCl) containing Complete, EDTA-free protease inhibitor (Roche) and 0.7 μg/ml pepstatin A (Sigma) and disrupted by passage 20 times through a 21-G needle. The cell sample was then centrifuged (2,000 rpm, 2 min, 4°C). The resulting supernatant was then centrifuged again (49,000 rpm, 30 min, 4°C; Optima MAX-E ultracentrifuge; Beckman Coulter). The pellet formed was dissolved in TBS containing Complete, EDTA-free protease inhibitors, 0.7 μg/ml pepstatin A, and 1% Triton X-100; incubated on ice for 1 hr; and ultracentrifuged again. The resulting supernatant will be referred to as the *membrane fraction*.

### Enzymatic Deglycosylation

The membrane fraction was solubilized with 1% Triton X-100 and then deglycosylated through treatment with the following: 1) endoglycosidase H (endo H; BioLabs), according to the manufacturer's instructions, and 2) 1 U N-glycosidase F (Endo F; Roche) per 45 μg of protein. The membrane fraction was denatured by boiling for 3 min in 1% SDS and 2-mercaptoethanol (ME), suspended in a reaction buffer (50 mM EDTA, 1% 2-ME, 0.5% Triton X-100, 0.1% SDS, 1 U N-glycosidase F) containing Complete, EDTA-free protease inhibitors and 0.7 μg/ml pepstatin A and incubated at 37°C overnight.

### Isolation of Lipid Rafts by Sucrose Density Gradient Centrifugation

Cells were lysed on ice in MBS buffer (25 mM MES, pH 6.5, 150 mM NaCl) containing 1% Triton X-100, Complete, EDTA-free protease inhibitors, and 0.7 μg/ml pepstatin A. Cell disruption was achieved by passing the lysate 10 times through a 21-G needle and then 20 times through a 27-G needle. The lysate was incubated at 4°C for 30 min, and an equal amount of 80% sucrose was then added to it. The sample and sucrose buffer, containing 5–40% sucrose, were sequentially loaded to the bottom of a tube and then centrifuged (36,000 rpm, 18 hr, 4°C; CP 70 WX ultracentrifuge; Hitachi). Fractions were collected from the top to the bottom. Equal volumes of these samples were analyzed by Western blotting.

### Methyl-β-Cyclodextrin Treatment

HEK293 cells overexpressing FLAG NEP-WT were washed with PBS, treated with 10 mM methyl-β-cyclodextrin (MβCD; Trappsol) for 20 min in a $CO_2$ incubator at 37°C, and collected. Lipid rafts fractions were treated with 50 mM MβCD on ice for 1 hr, dissolved in a double volume of TBS containing Complete, EDTA-free protease inhibitors and 0.7 μg/ml pepstatin A, and centrifuged (49,000 rpm, 1 hr, 4°C). The supernatants were removed and the pellets dissolved in TBS.

### Western Blotting

Equal amounts of protein samples were separated by SDS-PAGE or Blue Native-PAGE and transferred to Immobilon-P PVDF membranes (Millipore, Billerica, MA). In the case of Blue Native-PAGE, the membranes were washed and destained using methanol. The membranes were soaked in PBS containing 5% nonfat dried milk and 0.05% Tween for 1 hr and then incubated overnight at 4°C with primary antibodies diluted in PBS containing 0.05% Tween, 0.1% BSA, and 1 mM $NaN_3$. After washing, the membranes were incubated with HRP-conjugated secondary antibody for 1 hr. Antigen–antibody complexes were detected by enhanced chemiluminescence using a LAS-3000 Luminescent Image Analyzer (Fujifilm). Signals were quantified in MultiGauge software (version 2.3; Fujifilm).

### Assay of NEP-Dependent Neutral Endopeptidase Activity

NEP activity was measured in vitro by incubation at 37°C for 1 hr in 100 mM MES (pH 6.8) containing Complete, EDTA-free protease inhibitors, 10 μM Z-Leu-Leu-Leu-H, and as a substrate 50 μM Z-Ala-Ala-Leu-*p*-nitroanilide (ZALL-*p*-NA; Peptide Institute), in the presence or absence of 10 μM thiorphan, a specific inhibitor of NEP.

### Interaction of NEP With Various Lipids

Lipid-spotted membrane (P-6002; Echelon Biosciences) was treated with TBS containing 1% skim milk and gently

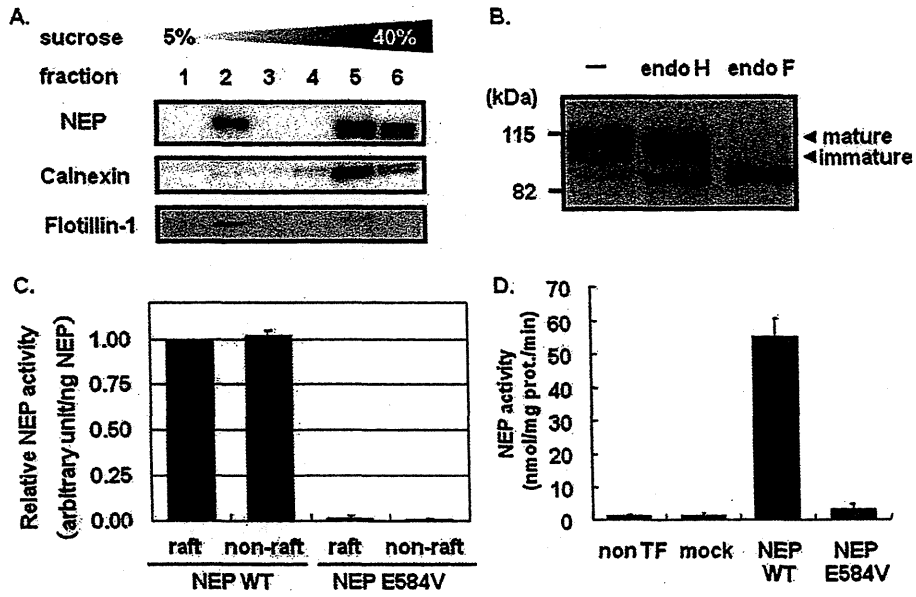


Fig. 1. NEP localization and activity in lipid rafts. **A:** Western blot analysis of lipid rafts fractionated from HEK293 cells overexpressing FLAG-NEP WT by a sucrose density-gradient centrifugation method. An anti-FLAG antibody was used to detect NEP. Lipid rafts were detected using an antibody raised against the raft marker flotillin-1. Nonlipid rafts (fraction 5) were detected using an antibody raised against the nonraft marker calnexin. **B:** Deglycosylation of the membrane fraction prepared from HEK293 cells overexpressing FLAG-NEP WT. The membrane fraction was treated with endoglycosidase H (endo H) and endoglycosidase F (endo F) or left untreated as a control (–), and then analyzed by Western blotting with an anti-FLAG antibody. **C:** Comparison of the specific enzymatic activity of the mature form NEP in lipid rafts (fraction 2) and nonlipid rafts (fraction 5), as assessed by *p*-NA peptide assay. Values represent the mean ± SD of three experiments. **D:** Neprilysin-dependent neutral endopeptidase activity in membrane fractions prepared from nontransfected HEK293 cells (non-TF) and cells transfected with vector (mock), FLAG-NEP WT (NEP WT) or the catalytically inactive mutant FLAG-NEP E584V. Values represent the mean ± SD of three experiments.

agitated for 1 hr at room temperature. SH-SY5Y neuronal cells were fractionated by sucrose density gradient centrifugation as shown previously, and each fraction was added to an equal volume of TBS containing protease inhibitor cocktail. After centrifugation at 49,000 rpm for 1 hr, the precipitate was dissolved in TBS containing protease inhibitor cocktail and incubated with the P-6002 membrane for 1 hr at room temperature. After incubation, the membrane was washed with TBS containing 0.1% Tween three times and incubated with anti-NEP monoclonal antibody diluted 1:2,000 for 1 hr at room temperature. The bound NEP was detected with an ECL advance kit (GE Healthcare, Amersham, United Kingdom).

## RESULTS

### Localization and Peptidase Activity of NEP in Lipid Rafts

To evaluate the peptidase activity of NEP in lipid rafts, we fractionated lipid rafts by sucrose density gradient centrifugation. We analyzed the localization of membrane-bound NEP extracted from HEK293 cells overexpressing FLAG-NEP WT. A raft marker, flotillin-1, was detected in fraction 2 and a nonraft marker, calnexin, in fractions 5 and 6 (Fig. 1A). FLAG-NEP was detected as a single band in fraction 2 and doublet bands in fractions 5 and 6. To distinguish these doublet bands, we deglycosylated the membrane fraction by treating it with endoglycosidase H (endo H) and endoglycosidase F (endo F; Fig. 1B). Although the upper band, the mature form, was resistant to endo H treatment, the lower band was deglycosylated by endo H. We will refer to the latter as the *immature form* of NEP. Resistance to endo H is acquired on transport of the protein to the Golgi apparatus, and this glycosylation is important for the catalytic activity of NEP (Lafrance et al., 1994). We compared the specific enzymatic activity of the mature form of NEP in lipid rafts (fraction 2) and nonlipid rafts (fraction 5); the contents of mature NEP were equalized by densitometric measurement of mature NEP levels after immunoblotting with an anti-FLAG antibody. The NEP activities of fractions 2 and 5, as assessed by *p*-NA peptide assay, were comparable (Fig. 1C). In this assay, catalytically inactive NEP E584V was used as a negative control (Fig. 1D).

### Localization of NEP in Lipid Rafts Is Dependent on Cholesterol

Only mature NEP was detected in lipid rafts (Fig. 1A). We thus hypothesized that cholesterol in lipid rafts regulated the localization of mature NEP. To test this, we depleted HEK293 cells overexpressing FLAG-NEP

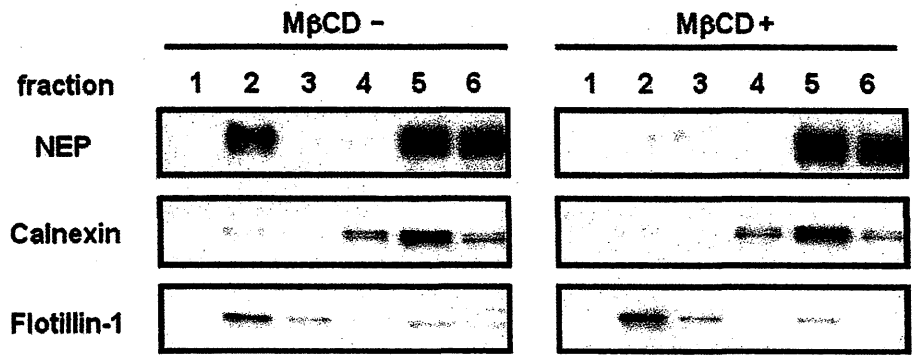


Fig. 2. Delocalization of NEP from lipid rafts in cells treated with MβCD. HEK293 cells overexpressing FLAG-NEP WT were treated with methyl-β-cyclodextrin (MβCD; +) or left untreated (–), and lipid rafts were fractionated as described in Materials and Methods.

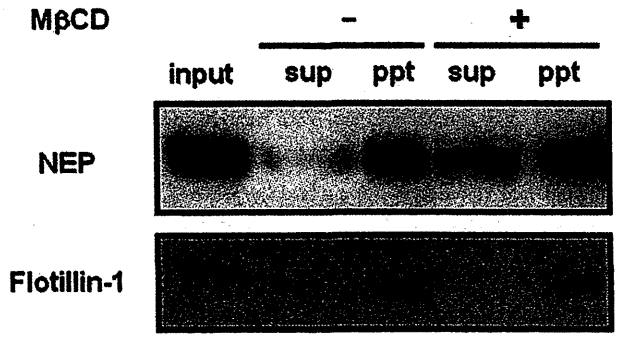


Fig. 3. Delocalization of NEP from fractionated lipid rafts after MβCD treatment. The lipid raft fraction, isolated from HEK293 cells overexpressing FLAG-NEP WT, was treated with (+) MβCD or left untreated (–) and separated into a supernatant (Sup) and a pellet (Ppt) by ultracentrifugation. The distribution of NEP was determined by Western blotting with an anti-FLAG antibody.

WT of cholesterol by treating them with 10 mM methyl-β-cyclodextrin (MβCD) for 20 min, and then fractionated the lipid rafts. More than 50% of cholesterol can be depleted from HEK293 cells by this treatment (Kojro et al., 2001). NEP became delocalized from lipid rafts following MβCD treatment, although flotillin-1 remained associated with them (Fig. 2).

We confirmed that the in vitro depletion of cholesterol from the lipid rafts fraction caused the delocalization of NEP from lipid rafts. We treated the fractionated lipid rafts with 50 mM MβCD for 1 hr at 4°C and separated them into supernatants and pellets by ultracentrifugation (Fig. 3). NEP and flotillin-1, associated with lipid rafts, were detected, as expected, in the pellets formed from lipid rafts not treated with MβCD. However, some of the NEP associated with lipid rafts was detected in supernatants prepared from lipid rafts treated with MβCD treatment. Flotillin-1 remained exclusively in the pellets, suggesting that flotillin-1 was not associated with choresterol.

## Localization of NEP in Lipid Rafts Is Enhanced by Its Dimerization

To understand better the mechanism of NEP localization in lipid rafts, we investigated whether NEP dimerization facilitated the assembly of the enzyme in lipid rafts. We lysed HEK293 cells overexpressing FLAG-NEP WT in buffers containing different detergents and then analyzed NEP protein complexes by Blue Native-PAGE. Although NEP complexes were dissociated by NP-40 and Triton X-100, the 300-kDa complexes were resistant to treatment with DDM and digitonin (Fig. 4A). Next, we investigated the effect of dimerization on the localization of NEP in lipid rafts. It has been reported that rabbit NEP carrying an E403C mutation forms a covalent homodimer (Hoang et al., 1997). We introduced this mutation into human NEP and assessed its effect on the localization of NEP in lipid rafts. FLAG-NEP WT and FLAG-NEP E403C were detected as single 120-kDa bands after their separation by SDS-PAGE under reducing conditions (Fig. 4B). A 250-kDa FLAG-NEP E403C homodimer was detected under nonreducing conditions (Fig. 4B). These results indicate that, as in rabbit NEP, the E403C mutation caused human NEP to form of a covalent homodimer. Interestingly, although NEP WT complexes (Fig. 4A,C) were not resistant to Triton X-100, the NEP E403C mutant was resistant to Triton X-100 and formed a disulfide-bonded complex the same size as the NEP WT complex. Although we cannot exclude the possibility that the complex includes other proteins, the 300-kDa complex (Fig. 4A,C) appears to represent a covalent NEP homodimer.

Next, we compared the localization of mature forms of NEP WT and NEP E403C in lipid rafts. The ratio of the amount of mature NEP localized in lipid rafts to the total amount of mature NEP was 1.3 times higher in HEK293 cells overexpressing homodimeric mutant NEP E403C (47.7%) than in those expressing NEP WT (35.7%; Fig. 4D). These results demonstrate that the localization of NEP in lipid rafts was enhanced by its dimerization.

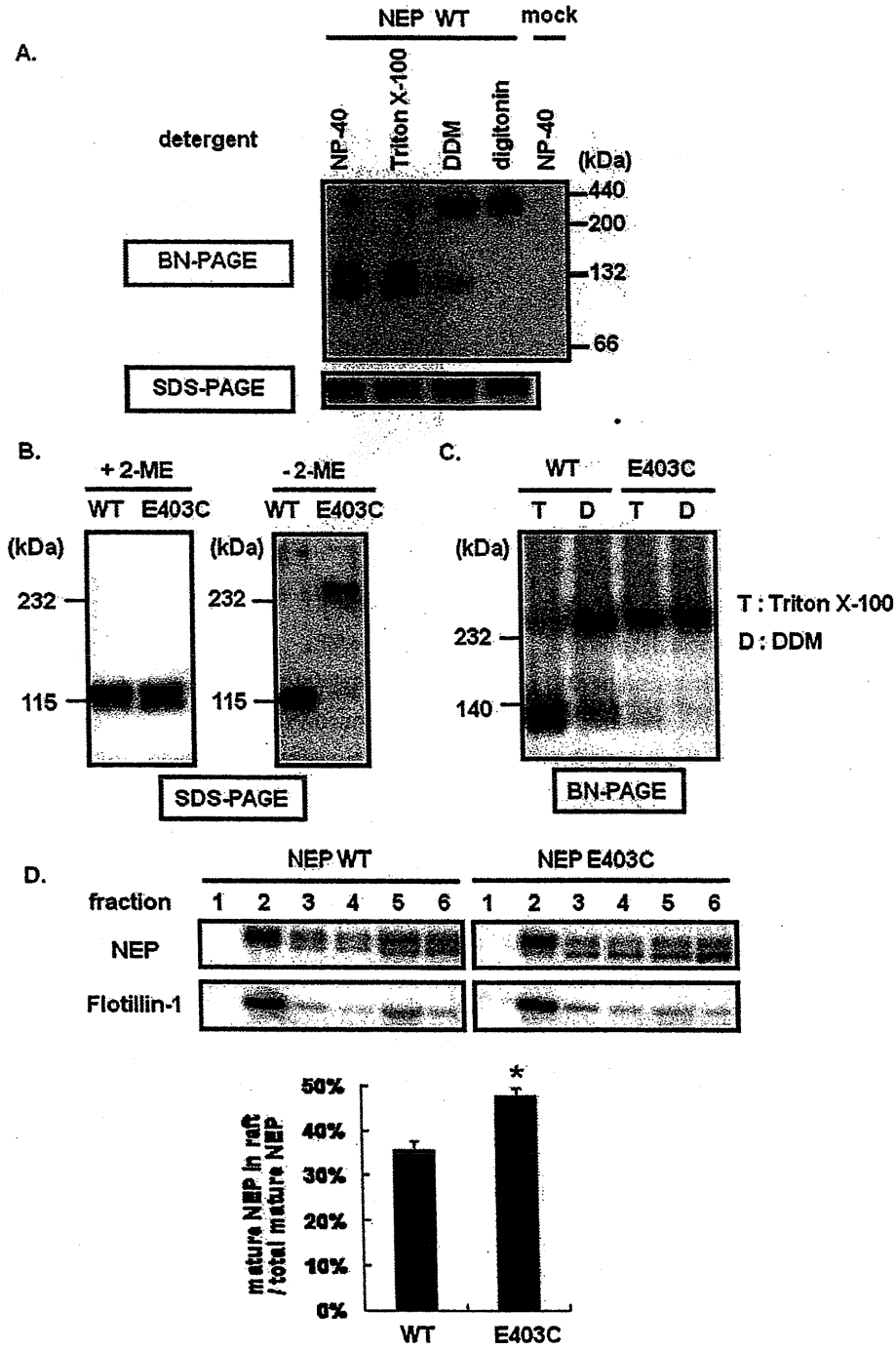


Fig. 4. Dimerization and localization of human NEP E403C in lipid rafts. **A:** Membrane fractions prepared from HEK293 cells overexpressing FLAG-NEP WT (NEP WT) or vector (mock) were dissolved in buffer containing detergents, such as NP-40, Triton X-100, DDM, and digitonin (all at a concentration of 1%). NEP complexes were analyzed by Blue Native-PAGE (BN-PAGE) or SDS-PAGE, followed by Western blotting with an anti-FLAG antibody. **B:** Membrane fractions obtained from HEK293 cells overexpressing FLAG-NEP WT (WT) or FLAG-NEP E403C (E403C) were analyzed by SDS-PAGE, performed with (**left**) or without (**right**) 2-ME. **C:** Membrane fractions obtained from HEK293 cells overexpressing FLAG-NEP WT (WT) or FLAG-NEP E403C (E403C) were dissolved in buffer containing 1% Triton X-100 (T) or 1% of DDM (D). The resulting lysates were analyzed by Blue Native-PAGE (BN-PAGE) and Western blotting with an anti-FLAG antibody. **D:** Effect of the E403C mutation on the distribution of NEP in lipid rafts. Lipid rafts from HEK293 cells overexpressing FLAG-NEP WT (NEP WT) or FLAG-NEP E403C (NEP E403C) were fractionated by sucrose density-gradient centrifugation and analyzed by Western blotting with an anti-FLAG antibody. The ratio of the amount of mature NEP localized in lipid rafts to the total amount of mature NEP was determined by densitometric measurement of protein bands corresponding to the mature form of NEP. Values represent the mean ± SD of three experiments. Statistical analysis was performed using a two-tailed Student's *t*-test. $*P < 0.05$ was considered to indicate statistical significance (bottom graph).